Primordial Magnetic Fields & Structure Formation In the Early Universe

Department of Physics, IIT-M, Chennai

Friday, June 14, 2013

Kanhaiya Lal Pandey
PhD Student
Under the Supervision of
Prof. Shiv K. Sethi

Astronomy & Astrophysics Group
Raman Research Institute, Bangalore, India

A Brief Outline

- Effect Of Primordial Magnetic Fields On Structure Formation In The Early Universe
  - **Formation Of High Red Shift Luminous Quasars (Super Massive Black Holes)**
- Probing Primordial Magnetic Fields by Studying the distribution of Mass In The Universe
  - **Constraints On Primordial Magnetic Fields Coming From Faraday Rotation of CMB Polarization Plane & Large Scale Structures**
  - **Constraints On Primordial Magnetic Fields Coming From Analysis Of Weak Lensing Shear**
  - **Constraints On Primordial Magnetic Fields Coming From Analysis Of Lyα Observables**

Publications

1. Supermassive Black Hole Formation At High Redshifts Through A Primordial Magnetic Field,

   Shiv K. Sethi, Zoltan Haiman, *Kanhaiya L. Pandey*
   2010, ApJ 721, 615

2. Primordial Magnetic Field Limits From Cosmological Data,

   Tina Kahniashivili, Alexander G. Tevzadze, Shiv K. Sethi,
   Kanhaiya L. Pandey, Bharat Ratra
   2010, PRD 82, 083005

3. Theoretical Estimates Of Two-point Shear Correlation Functions Using Tangled Magnetic Fields,

   Kanhaiya L. Pandey, Shiv K. Sethi
   2012, ApJ 748, 27

4. Probing Primordial Magnetic Fields Using Lyα Clouds,

   Kanhaiya L. Pandey, Shiv K. Sethi
   2012, ApJ 762, 15

Introduction

# #

[Primordial Magnetic Field & Its Effects On Structure Formation]

Magnetic Fields in the Universe / Cosmology

Observations

Observations of magnetic fields inside galaxies and clusters of galaxies even in ICM & IGM and high redshift galaxies tells us about the existence of magnetic fields in the universe which are coherent over very large scale and are substantially strong.

M51 (4.8 Ghz)

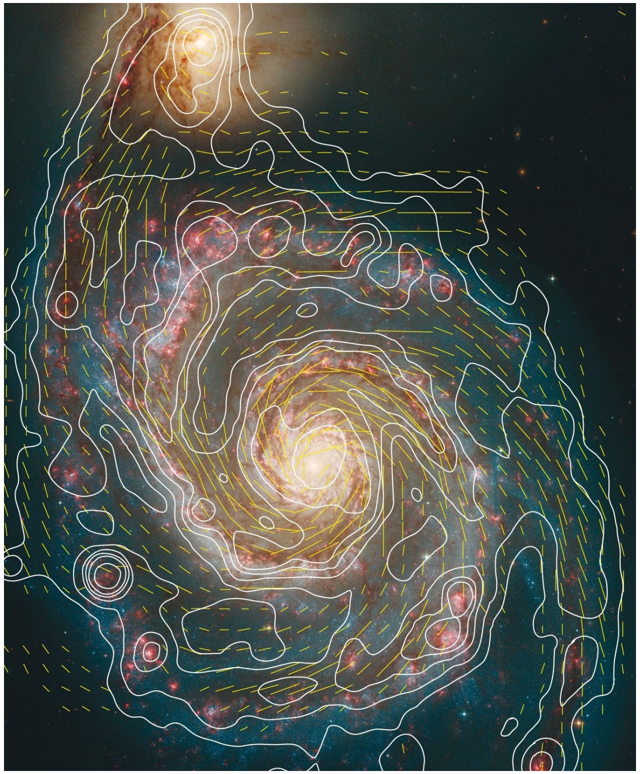

NGC891 (8.4 GHz)

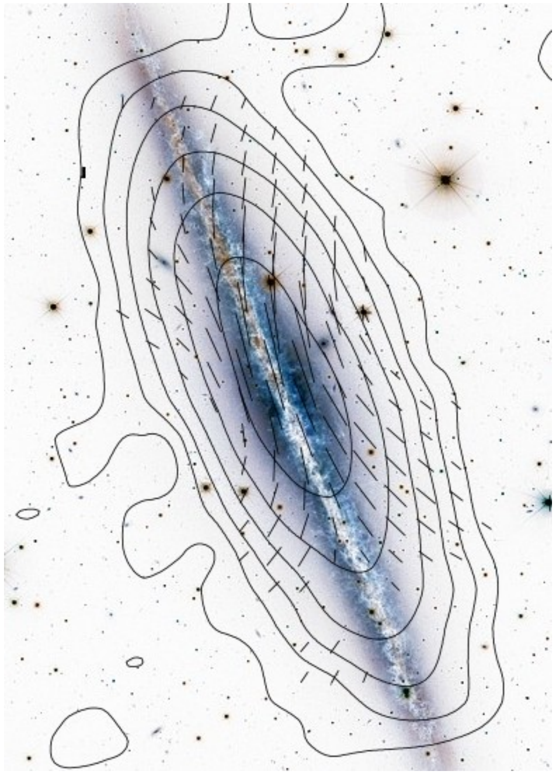

NGC4569 (4.8 GHz)

Pictures: Max Planck Institute for RadioAstronomy ; http://www.mpifr-bonn.mpg.de/staff/rbeck/MKSP/pictures.html

Magnetic Fields in the Universe / Cosmology

Primodial Magnetic Fields were first introduced to understand the large scale galactic magnetic fields

Are the observed cosmic magnetic fields actually result of some battery mechanism and the dynamo action (dynamo theory), or has it been there since almost beginning, generated much earlier, before the galaxy/clusters were formed (primordial magnetic field) ??

- *Post-Recombination Era : Biermann battery :* $B_0 \sim (10^{-20} - 10^{-18})$ **G**
- *PMF : during Inflation : vacuum fluctuations :* $B_0 \sim 10^{-9}$ **G**
- *The currently observed field strengths are of the order of* 10^{-6} **G**

Primordial magnetic field with a strength of even $B \sim 10^{-9}$ G (value redshifted to present epoch) and coherent on Mpc scales in the IGM could also be sheared and amplified due to flux freezing, during the collapse to form a galaxy and lead to the few μG field observed in disk galaxies.

primordial origin or dynamo : the picture is still not very clear

Magnetic Fields in the Universe / Cosmology

Modelling the Primordial Magnetic Fields

Let us start with assuming that some proccesses in the early universe led to the formation of primordial (tangled) magnetic fields, and which were initially

- ☛ *isotropic and homogeneous random distribution, the 2p corr. fn. -*

$$\left\langle \tilde{B}_i(\boldsymbol{q})\tilde{B}_j^*(\boldsymbol{k})\right\rangle = \delta_D^3(\boldsymbol{q} - k)\left(\delta_{ij} - k_i k_j/k^2\right) M(k)$$

where $M(k) = Ak^n$ *with cut off at* $k = k_{max}$

these mag. fields simply redshift as (in the linear regime)

$$\boldsymbol{B}(\boldsymbol{x}, t) = \tilde{\boldsymbol{B}}(\boldsymbol{x})/a^2$$

Sethi & Subramanian 2005

Structure Formation under the influence of Primordial Magnetic Field

Perturbations Generated in the Presence Of PMF

MHD eq^{n}s in co-moving coordinates in the linearized Newtonian theory

$$
\begin{aligned}
\frac{d(a\mathbf{v}_b)}{dt} &= -\nabla\phi + \frac{(\nabla\times\mathbf{B})\times\mathbf{B}}{4\pi\rho_b} \\
\nabla.\mathbf{v}_b &= -a\dot{\delta}_b \\
\nabla^2\phi &= 4\pi G a^2(\rho_{DM}\delta_{DM} + \rho_b\delta_b)
\end{aligned}
$$

→

$$\frac{\partial^2\delta_b}{\partial t^2} + 2\frac{\dot{a}}{a}\frac{\partial\delta_b}{\partial t} - 4\pi G(\rho_{DM}\delta_{DM} + \rho_b\delta_b) = \frac{\nabla.[(\nabla\times\mathbf{B})\times\mathbf{B}]}{4\pi a^2\rho_b}$$

$$
\begin{aligned}
\frac{\partial(a^2\mathbf{B})}{\partial t} &= \frac{\nabla\times(\mathbf{v}_b\times a^2\mathbf{B})}{a} \\
\nabla.\mathbf{B} &= 0
\end{aligned}
$$

→

$$\mathbf{B}(x,t)a^2 = \text{constant.}$$

source term from magnetic fields

$$\frac{\partial^2\delta_m}{\partial t^2} = -2\frac{\dot{a}}{a}\frac{\partial\delta_m}{\partial t} + 4\pi G\rho_m\delta_m + \frac{\rho_b}{\rho_m}S(t,x)$$

where

$$
\begin{aligned}
\delta_m &= (\rho_{DM}\delta_{DM} + \rho_b\delta_b)/\rho_m \\
\rho_m &= (\rho_{DM} + \rho_b)
\end{aligned}
$$

Structure Formation under the influence of Primordial Magnetic Field

growth of perturbations; various sacles in the problem

cut off scale λ_{max} $(\sim v_A L_S)$ *, due to damping by radiative viscosity before recombination*

$$k_{\rm max} \simeq 235\,{\rm Mpc}^{-1} \left(\frac{B_{\rm m}}{10^{-9}\,{\rm G}}\right)^{-1} \left(\frac{\Omega_{\rm m}}{0.3}\right)^{1/4} \times \left(\frac{\Omega_{\rm b}h^2}{0.02}\right)^{1/2} \left(\frac{h}{0.7}\right)^{1/4}$$

magnetic field Jeans Length λ_J *, due to magnetic pressure after recombination*

$$k_{\rm J} \simeq 14.8\,{\rm Mpc}^{-1} \left(\frac{\Omega_{\rm m}}{0.3}\right)^{1/2} \left(\frac{h}{0.7}\right) \left(\frac{B_{\rm J}}{10^{-9}\,{\rm G}}\right)^{-1}$$

$$\lambda_J = \frac{2\pi}{k_J} = v_A \sqrt{\frac{\pi}{\rho G}}$$

$$v_A = \frac{B}{\mu_0 \rho}$$

where $B_{\rm J} = B(k_{\rm J},\ t)\ a^2(t)$ *and* $B_{\rm J} = B_{\rm G}(k_{\rm J}/k_{\rm G})^{(n+3)/2}$

dissipation of primordial tangled magnetic fields in the post recombination era also results in an increase in the "Thermal Jeans Length"

Sethi & Subramanian 2005

Structure Formation under the influence of Primordial Magnetic Field

Matter Power Spectrum due to Primordial Magnetic Field

for the initial density perturbations which were caused by, then present, primordial magnetic fileds, the theoratical expression for the density power spectrum takes the form -

$$P(k) = \int_{k_{min}}^{k_{max}} dk_1 \int_{-1}^{+1} d\mu \frac{B^2(k_1)B^2(|\mathbf{k}-\mathbf{k_1}|)}{|\mathbf{k}-\mathbf{k_1}|^2}$$

$$\times \left[2k^5 k_1^3 \mu + k^4 k_1^4 (1-5\mu^2) + 2k^3 k_1^5 \mu^3\right]$$

where, $B^2(k) = Ak^n$ $\qquad A = \frac{\pi^2(3+n)}{k_c^{(3+n)}} B_0^2$

$$B_0^2 \equiv \langle B_i(\mathbf{x}, t_0) B_i(\mathbf{x}, t_0) \rangle = \frac{1}{\pi^2} \int_0^{k_c} dk \; k^2 B^2(k)$$

Gopal & Sethi 2004

Structure Formation under the influence of Primordial Magnetic Field

Matter Power Spectra

Power Spectrum for the magnetic and non magnetic cases. The green and red curves are for non magnetic case, with linear and nonlinear z evolution respectively. Other curves are the power spectra (linear) for magnetic cases with magnetic field strengths B_0 = 1 nG & 3 nG and mag. field spectral index n = -2.7 & -2.9 .

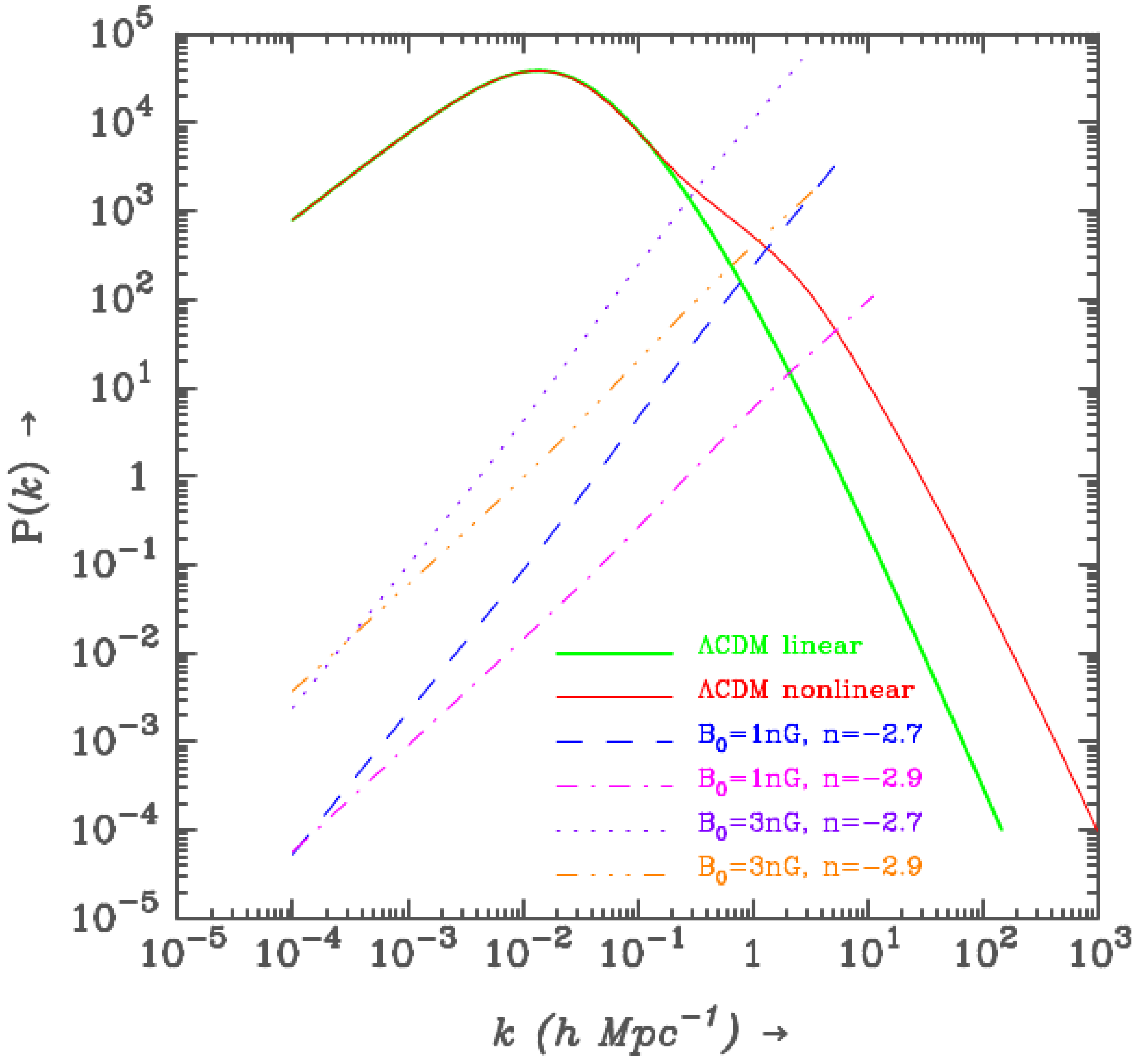

Effect Of Primordial Magnetic Fields On Structure Formation In The Early Universe

1

[Formation Of High Red-Shift Luminous Quasars (Super Massive Black Holes)]

Shiv K Sethi, Zoltan Haiman, *Kanhaiya Lal Pandey*

Formation Of High Red Shift Luminous Quasars (Super Massive Black Holes)

The Puzzle

From The Sloan Digital Sky Survey :

discovery of very bright quasars, $L \sim 10^{47}$ erg/s, @ redshift $z \sim 6$

↓

SMBHs $M \sim 10^9\ M_\odot$ already existed when the universe was less than 1 Gyr old !!

But How ??

$T_{eddington}$ ≈ *age of the Universe !!*

" *seed black holes*[§] " ————————————→ SMBH

§ *remnant from the early* ($z \approx 25$) *Pop III, 100* M_{Sun}, *metal free stars*

Formation Of High Red Shift Luminous Quasars (Super Massive Black Holes)

Challanges & Possible Explanations

☛ Rapid (metal-free) gas accretion in relatively massive ($\geq 10^8\ M_{sun}$, $T_{vir} \geq 10^4$ K) dark matter halos @ red shift z ~ 10

☛ The gas that cools and collapses in these halos

1. must avoid fragmentation,
2. shed angular momentum efficiently, and
3. collapse rapidly.

☛ These conditions are unlikely to be met unless the gas remains 'warm', i.e. At temperature $T_{vir} \geq 10^4$ K. (due to H_2 cooling in this scenario)

☛ Even if one considers photo-dissociation of H_2 or intermidiary H^- by UV background radiation from nearby galaxies, the critical flux needed comes out to be too high ..

Formation Of High Red Shift Luminous Quasars (Super Massive Black Holes)

If Primordial Magnetic Fields Play a role ....

dissipation of primordial magnetic field due to

1. ambipolar diffusion and
2. decaying turbulence

in the intergalactic medium (IGM) can actually heat the surrounding medium and thus inhibit H_2-cooling.

Formation Of High Red Shift Luminous Quasars (Super Massive Black Holes)

If Primordial Magnetic Fields Play a role ....

Chemistry And The Thermo-dynamical Evolution Of Collapsing Primordial Gas

- **Density evolution of the collapsing halo**

  1. Spherical Top Hat collapse of (dark + baryonic matter) till virialization
  2. Further collapse of baryonic matter inside virialized halo of dark matter (assumptions:
     1. isothermal dark matter halo profile,
     2. spherical collapse of baryonic matter, no shell crossing
     3. The prescription is based on energy conservation.

- **Thermal evolution of the collapsing gas**

  1. **Magnetic heating**

     Ambipolar diffusion + turbulent decay of magnetic fields

  2. **Other cooling (heating) processes**

     Compton cooling + HI line cooling + H_2 molecular cooling + adiabetic cooling/heating due to expansion/collapse

Formation Of High Red Shift Luminous Quasars (Super Massive Black Holes)

If Primordial Magnetic Fields Play a role ....

Chemistry And The Thermo-dynamical Evolution Of Collapsing Primordial Gas

the evolution of the ionization fraction (x_e), magnetic field energy density (E_B), temperature (T), and H_2 molecule fraction (x_{H2}) are described by the equations, -

$$
\begin{aligned}
\dot{x}_e &= \left[\beta_e(1-x_e)\exp\left(-h\nu_\alpha/(k_B T_{\rm cbr})\right) - \alpha_e n_b x_e^2\right] C + \\
&\quad + \gamma_e n_b (1-x_e) x_e \\
\frac{dE_B}{dt} &= \frac{4}{3}\frac{\dot{\rho}}{\rho} - \left(\frac{dE_B}{dt}\right)_{\rm turb} - \left(\frac{dE_B}{dt}\right)_{\rm ambi} \\
\frac{dT}{dt} &= \frac{2}{3}\frac{\dot{n}_b}{n_b} T + k_{iC} x_e (T_{\rm cbr} - T) + \frac{2}{3 n_b k_B}\left(L_{\rm heat} - L_{\rm cool}\right), \\
\frac{dx_{\rm H_2}}{dt} &= k_m n_b x_e (1 - x_e - 2x_{\rm H_2}) - k_{\rm des} n_b x_{\rm H_2}.
\end{aligned}
$$

Formation Of High Red Shift Luminous Quasars (Super Massive Black Holes)

If Primordial Magnetic Fields Play a role .. The Results ..

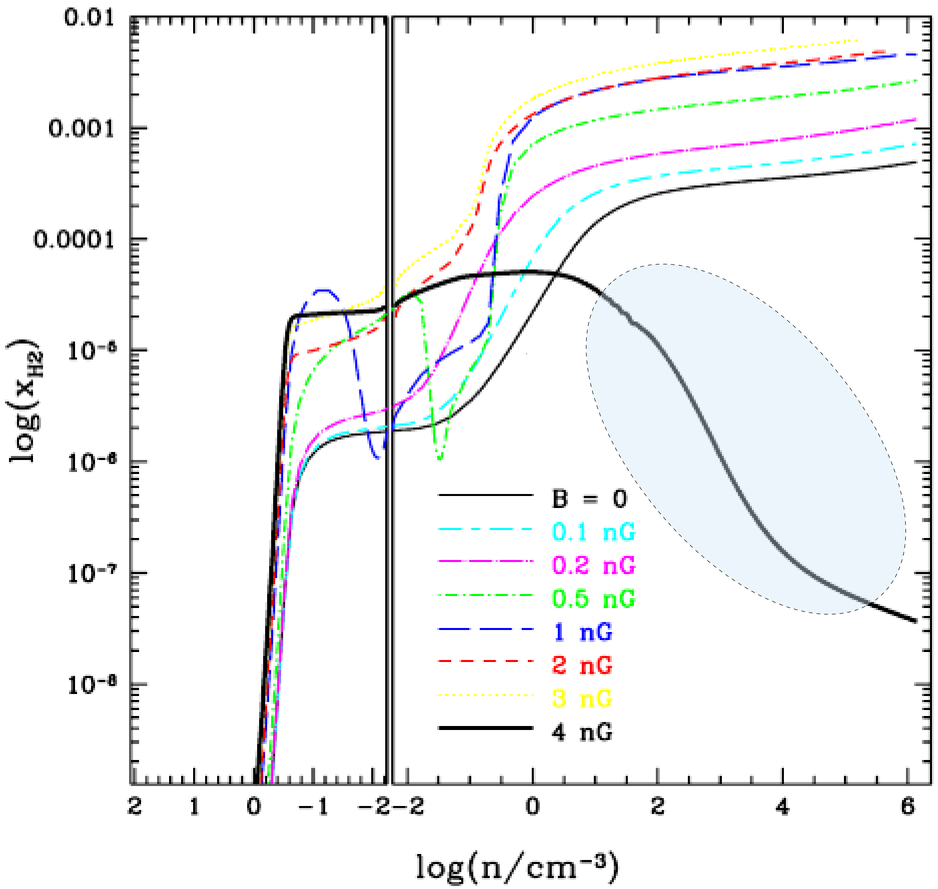

The evolution of the H2 fraction

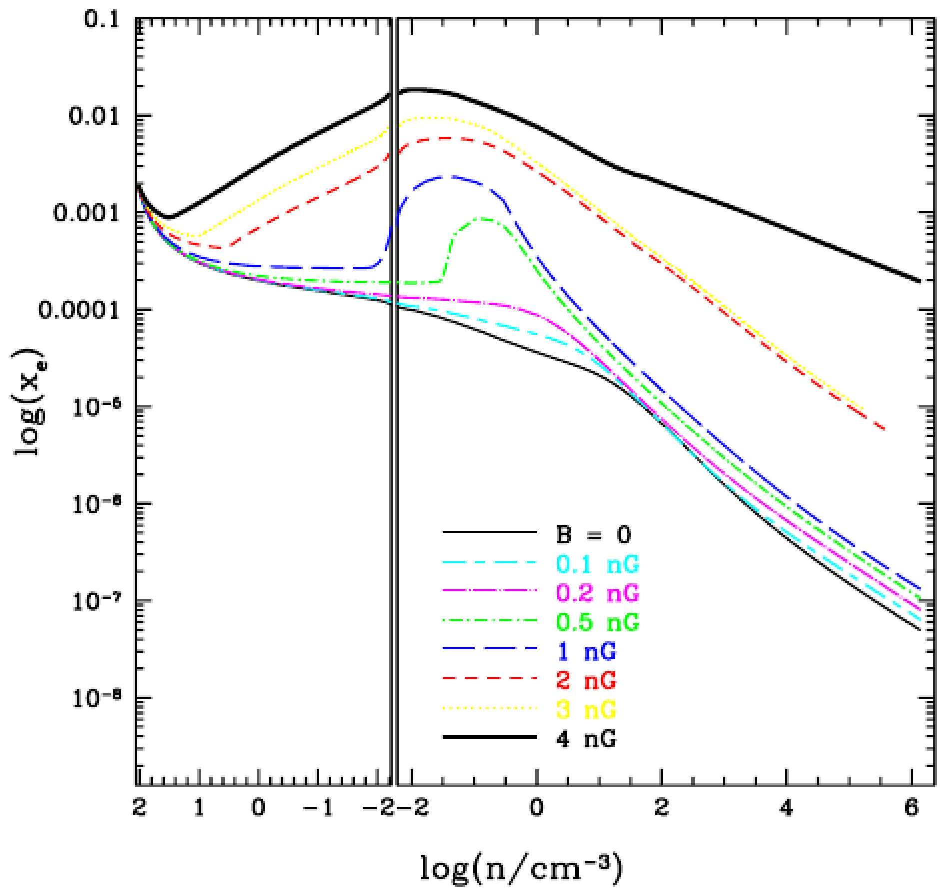

The evolution of the ionized fraction

Formation Of High Red Shift Luminous Quasars (Super Massive Black Holes)

If Primordial Magnetic Fields Play a role .. The Results ..

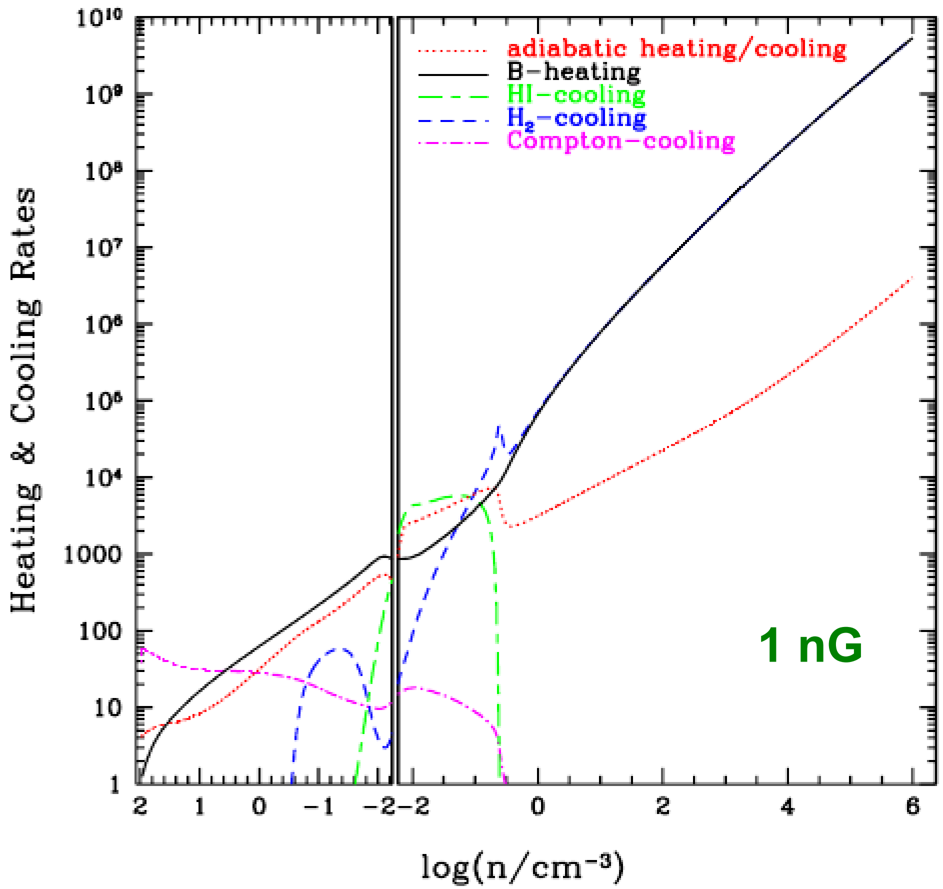

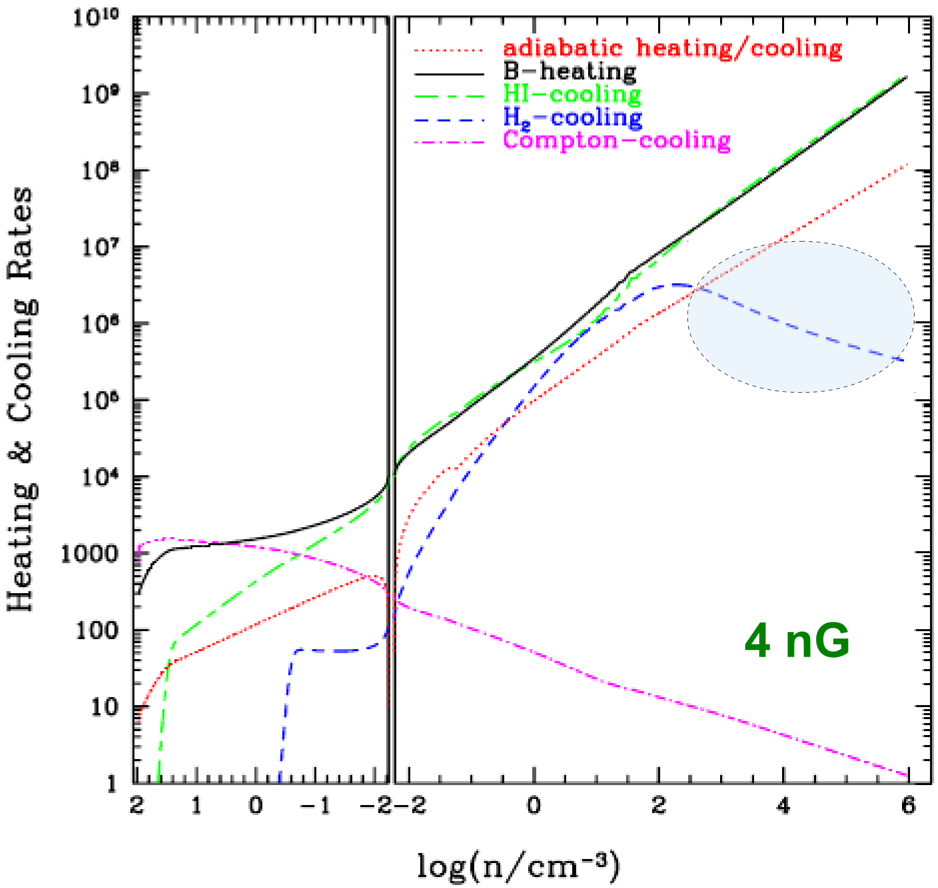

heating and cooling rates for various processes

Formation Of High Red Shift Luminous Quasars (Super Massive Black Holes)

If Primordial Magnetic Fields Play a role .. The Results ..

For B > B_{crit} ~ 3.5 nG , H2 cooling then remains inefficient, and the temperature stays near ~ 10^4 K, even as the gas collapses further.

If B < B_{crit} , H_2 cooling is delayed, and the gas eventually cools down below ~ 1000 K.

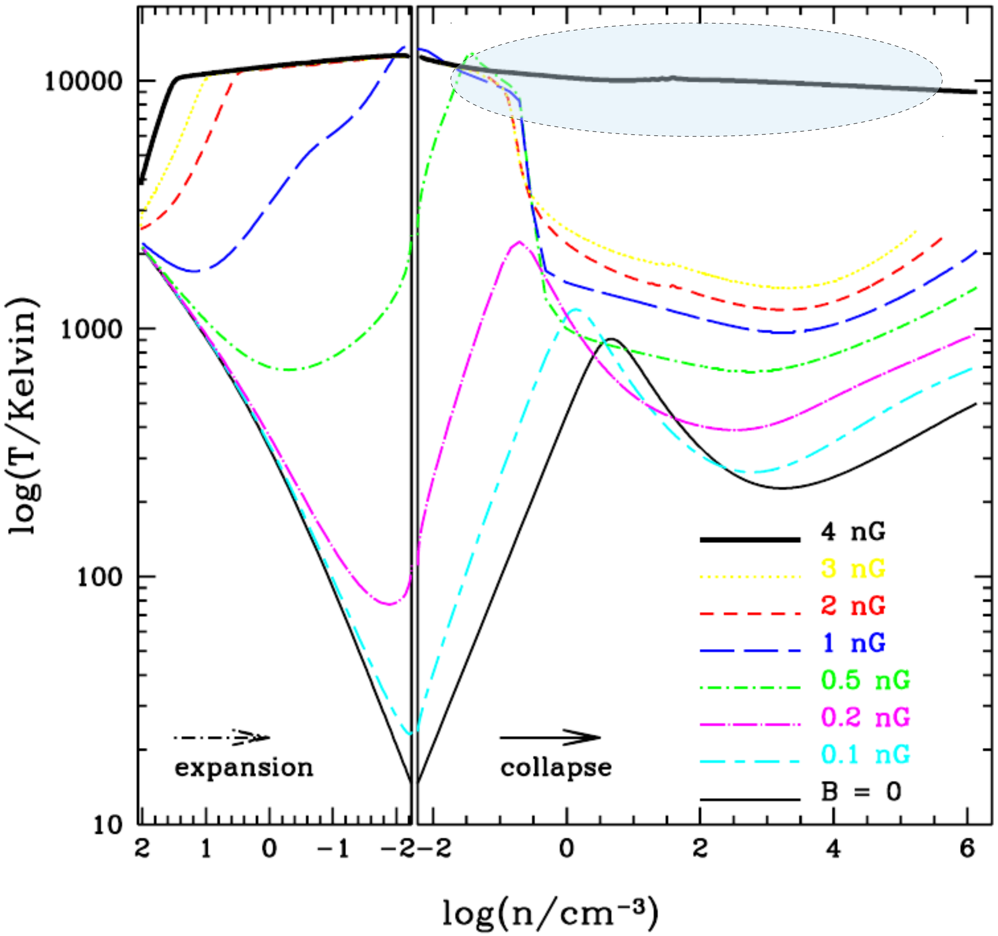

Formation Of High Red Shift Luminous Quasars (Super Massive Black Holes)

If Primordial Magnetic Fields Play a role .. The Results ..

The Mass of The Central Object : The expected mass of the central object scales approximately as

$$M \propto t_{acc}^{-1} \propto c_s^{3} \propto T^{3/2}$$

$200\ M_{Sun}$: $T = 300$ K : : $4\times10^{4}\ M_{Sun}$: $T \approx 10^{4}$ K.

$10^{9}\ M_{Sun}$

$z \sim 15$ to $z \sim 6$
enough time for Eddington limited growth

Formation Of High Red Shift Luminous Quasars (Super Massive Black Holes)

Results & Conclusions

- *Our calculations showed that the direct gas collapse in the early dark matter halos, aided by heating from the dissipation of a primordial magnetic field can lead to the formation of high mass objects which in turn can grow into a SMBH by the redshifts of 6-8.*

- *This model avoids many of the odd assumptions required in earlier models (such as an extremely high UV flux and the absence of H_2 and of other molecules and metals).*

- *But at the same time this model requires a large primordial magnetic field and relies on metal-free primordial gas.*

- *From this analysis, in general, it seems that any other heating mechanism, which could compete with atomic HI cooling in the collapsing halo, down to a density of $n \sim 10^3\ cm^{-3}$, would produce similar effect as the magnetic field produced here.*

Probing Primordial Magnetic Fields by Studying the distribution of Mass In The Universe

2

(Constraints On Primordial Magnetic Fields From The Faraday Rotation of CMB Polarization Plane & Large Scale Structure (LSS) Formation)

Tina Kahniashvili, Alexander G. Tevzadze, Shiv K Sethi,
Kanhaiya Lal Pandey and Bharat Ratra

PMF & CMB Polarization

The Faraday Rotation of CMB Polarization Plane

A quadrupole anisotropy in the temperature inhomogeneity can lead to polarization of CMB photons

The presence of a primordial magnetic field during recombination causes a rotation of the CMB polarization plane through the Faraday effect.

plane through the Faraday effect . The rms rotation angle $\alpha_{\rm rms} = (\langle \alpha^2 \rangle)^{1/2}$ induced by a stochastic magnetic field with smoothed amplitude B_λ and spectral index n_B is given by

$$\langle \alpha^2 \rangle = \sum_l \frac{2l+1}{4\pi} C_l^\alpha,$$

where the rotation multipole power spectrum C_l^α is

$$C_l^\alpha \simeq \frac{9l(l+1)}{(4\pi)^3 q^2 \nu_0^4} \frac{B_\lambda^2}{\Gamma(n_B/2+3/2)} \left(\frac{\lambda}{\eta_0}\right)^{n_B+3} \int_0^{x_S} dx x^{n_B} j_l^2(x).$$

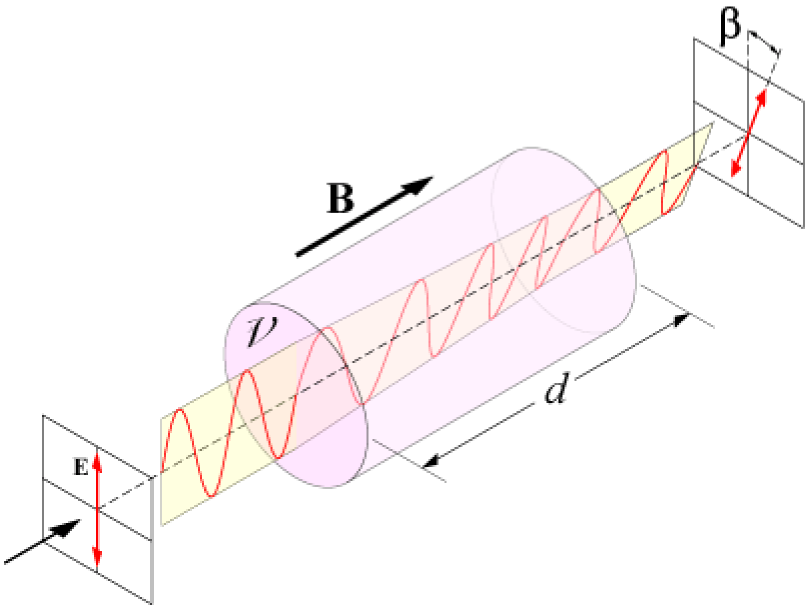

PMF & CMB Polarization

Constraints On PMF From the Faraday Rotation of CMB Polarization Plane

Effective magnetic field limits set by the measurement of the rotation angle α_{rms}.

The horizontal solid line shows the upper limit set by BBN.

Vertical dashed lines correspond to the $\alpha_{rms} = 3.16^\circ$ that is set by the BBN limit on the effective magnetic field with spectral index $n_B = 2$

$\alpha_{rms} = 4.4^\circ$ is set by the WMAP-7 year data.

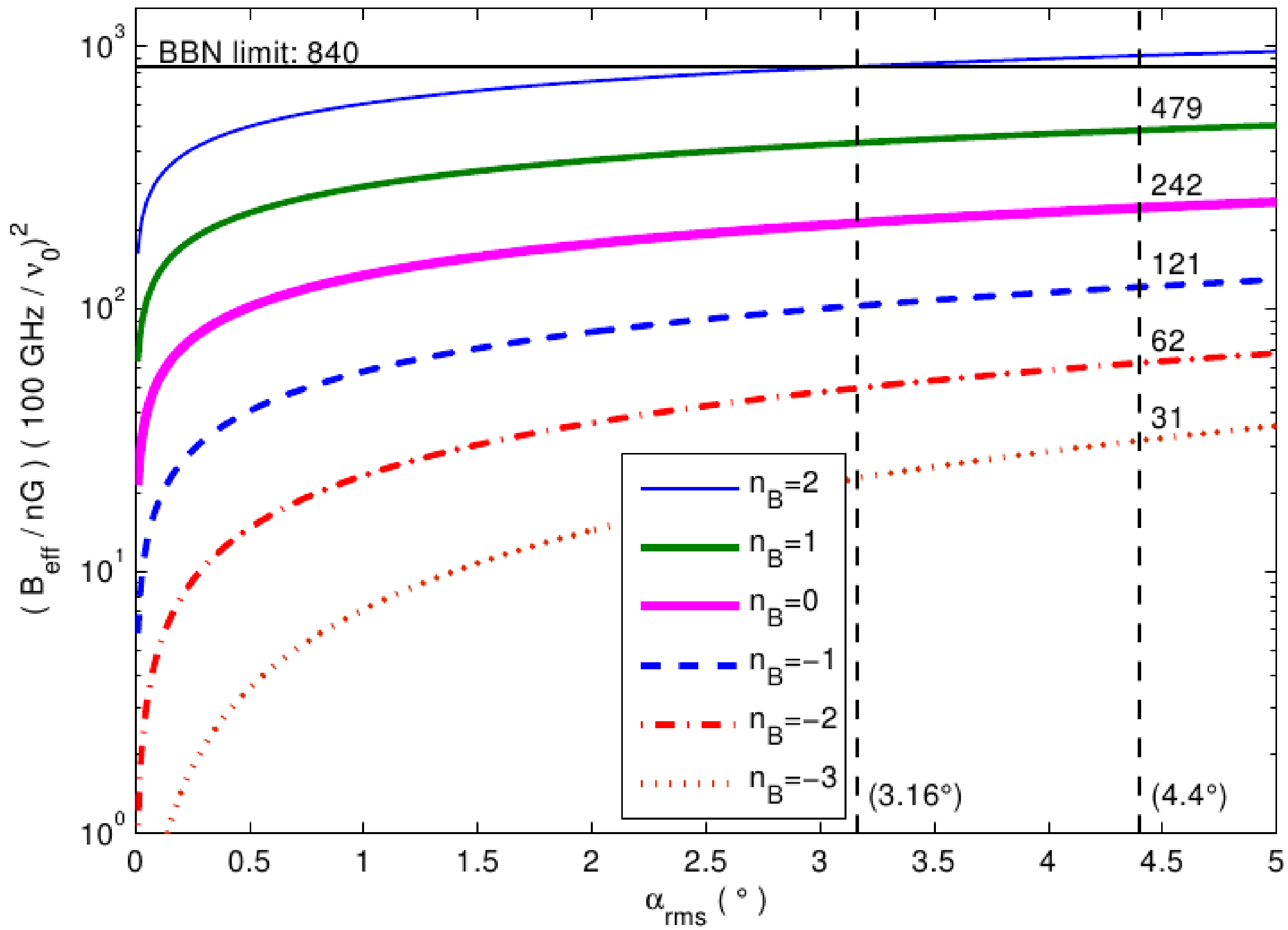

Constraints On PMF From the LSS

Mass dispersion vs Mass scale when the magnetic field induced matter power spectrum is added

Since the magnetic field induced matter perturbations are uncorrelated with the inflationary matter perturbations, the two power spectra can simply be added in quadrature.

From this figure many of the primordial magnetic field models with high spectral index (n_B) values are ruled out.

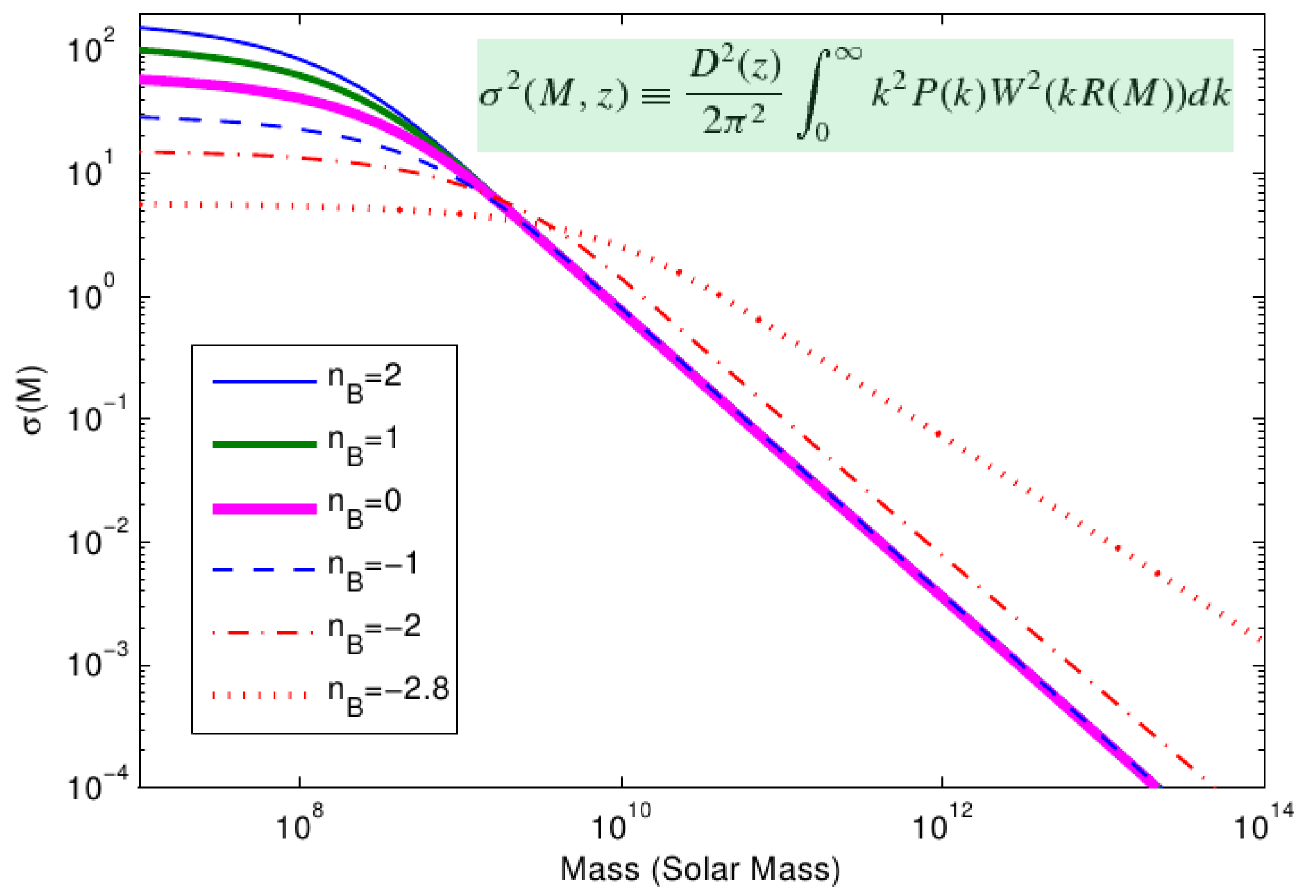

*The mass dispersion at **z = 10 for B_{eff} = 6 nG** as a function of n_B*

Constraints On PMF From the LSS

Results & Conclusions

- *Limits on B_{eff} using WMAP-7 bound on the rms rotation angle (4.4^o at 95% CL).*

- *The mass dispersion on small scales is larger for a larger value of n_B.*

- *For $n_B \geq -1.5$, the mass dispersion drops more sharply at larger scales than for $n_B \leq -1.5$.*

- *The smallest structures to collapse at $z \simeq 10$ in the WMAP-normalized ΛCDM model are 2.5σ fluctuations of the density field as opposed to the magnetic field case where 1σ collapse is possible. This means the number of collapsed halos is more abundant in the later case.*

Probing Primordial Magnetic Fields by Studying the distribution of Mass In The Universe

3

(Constraints On Primordial Magnetic Fields Coming From The Analysis Of Weak Lensing Signal)

Kanhaiya Lal Pandey, Shiv K Sethi

Constraints On PMF From Cosmic Shear Analysis

Weak Lensing & Cosmic Shear

Effect of lensing:

- isotropic magnification (convergence κ)
- anisotropic stretching (shear γ)

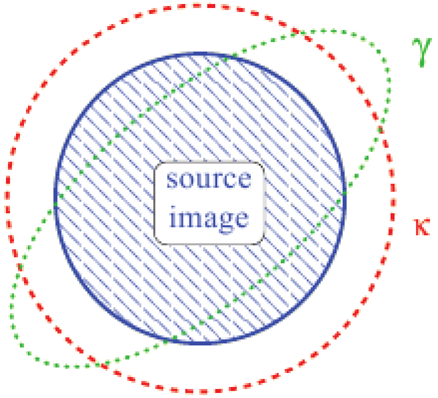

Weak lensing regime: $\kappa \ll 1$

$$\varepsilon^{\text{observed}} = \varepsilon^{\text{intrinsic}} + \gamma$$

$$\left\langle \varepsilon^{\text{observed}} \right\rangle = \gamma \qquad \text{since} \qquad \left\langle \varepsilon^{\text{intrinsic}} \right\rangle = 0$$

$$|\varepsilon| = \frac{1-b/a}{1+b/a}$$

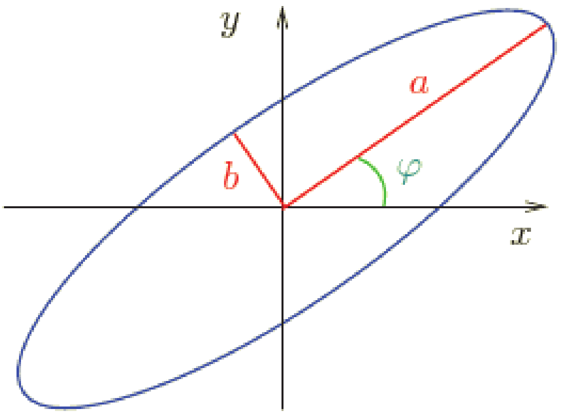

Figures : Martin Kilbinger, 2006

Constraints On PMF From Cosmic Shear Analysis

Weak Lensing & Cosmic Shear

Cosmic shear = the coherent distortion of images of distant galaxies caused by matter inhomogeneities on large scales.

Distortions lead to observable mutual alignment or correlation of orientation of background galaxy images.

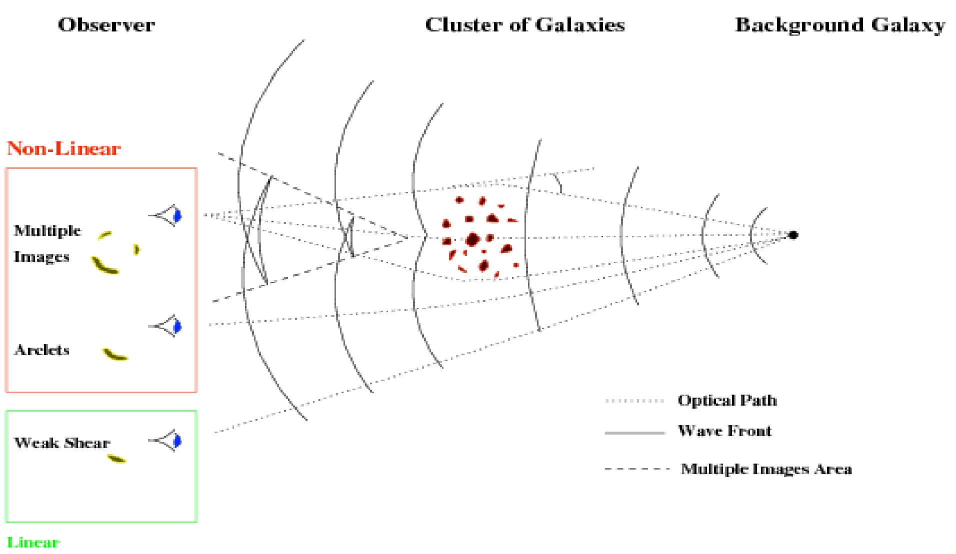

Cumulative distortion along the line of sight $\Longrightarrow$ sensitive to projected matter distribution or convergence κ.

Constraints On PMF From Cosmic Shear Analysis

Cosmic Shear Power Spectrum

Given matter power spectrum P_δ *, one can calculate shear power spectrum using following relation (limber's equation) .*

$$P_\kappa(\ell) = \frac{9}{4}\Omega_m^2 \left(\frac{H_0}{c}\right)^4 \int_0^{\chi_{lim}} \frac{d\chi}{a^2(\chi)} P_\delta\left(\frac{\ell}{f_K(\chi)};\chi\right) \times \left[\int_\chi^{\chi_{lim}} d\chi' n(\chi') \frac{f_K(\chi'-\chi)}{f_K(\chi')}\right]^2$$

where, $\chi(z) = \frac{c}{H_0}\int_0^z (\Omega_m(1+z)^3 + \Omega_\Lambda)^{-1/2} dz$

For spatially flat (K=0) universe $f_K(\chi) = \chi$

Constraints On PMF From Cosmic Shear Analysis

2-Point Shear Correlation Functions : the observables

We can decompose the observed shear signal into E (non-rotational) and B (rotational) components in general. These decomposed shear correlation functions are given by the following expression

$$\xi_{E,B}(\theta) = \frac{\xi_+(\theta) \pm \xi'(\theta)}{2}$$

where,

$$\xi'(\theta) = \xi_-(\theta) + \int_\theta^\infty \frac{d\vartheta}{\vartheta} \xi_-(\vartheta) \left(4 - 12\left(\frac{\theta}{\vartheta}\right)^2\right)$$

ξ_+ and ξ_- are again two-point shear correlation functions which are directly realted to the power spectrum according to the following equation,

$$\xi_\pm(\theta) = \frac{1}{2\pi} \int_0^\infty d\ell\ \ell P_\kappa(\ell) J_{0,4}(\ell\theta)$$

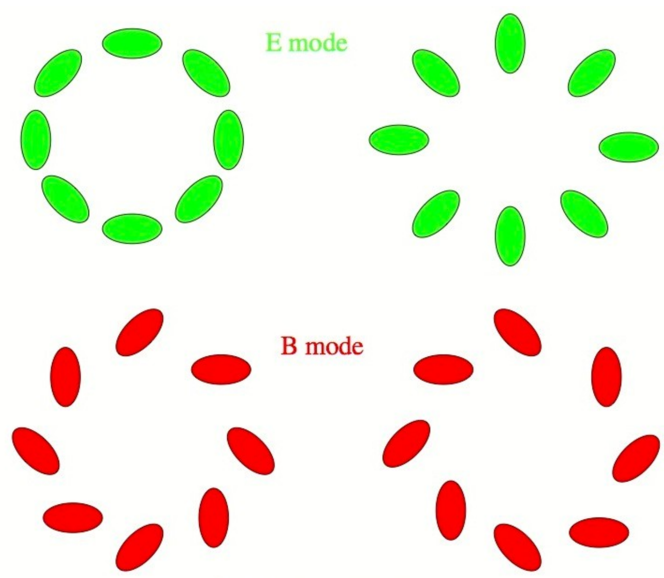

van Waerbeke & Mellier 2003

Schneider, Waerbeke & Melier 2002

Constraints On PMF From Cosmic Shear Analysis

Shear Power Spectra

Shear Power Spectra for the magnetic and non magnetic cases. Red and green curves represent the shear power spectra for non magnetic case and the blue & magenta curves represent the same for the magnetic cases (B_0 = 3nG & 1.0nG, n = –2.9), respectivly

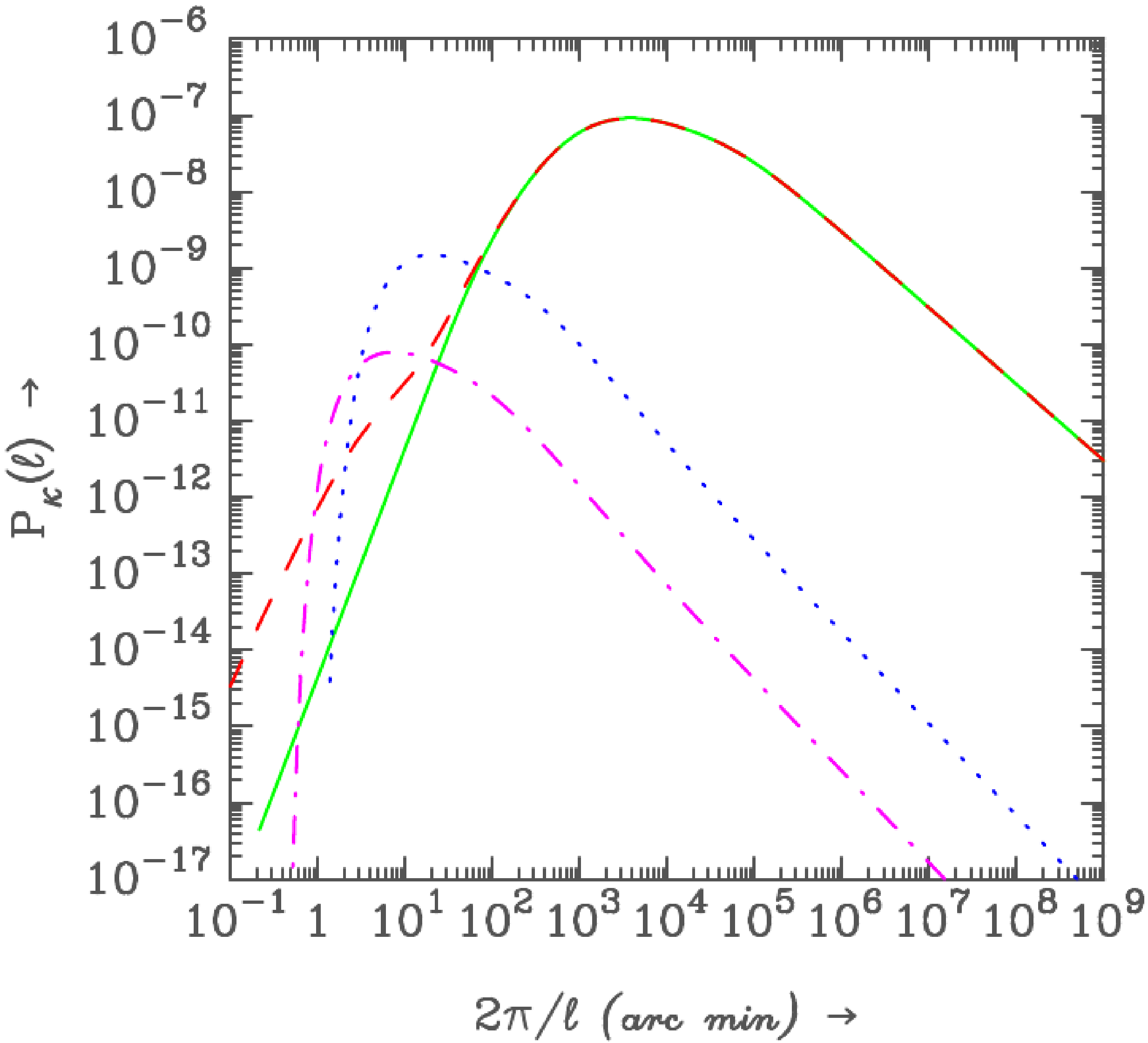

Constraints On PMF From Cosmic Shear Analysis

Decomposed two- point shear correlation functions $\xi_{E,B}$ for magnetic and non magnetic cases. Red curve represents the ξ_E for non magnetic case and the other bluish curves are the same for magnetic cases (B_0 = 1, 2 & 3 nG, n = –2.9). ξ_Bs for both the cases are almost zero. The orange and green curves with errorbars are the ξ_E and ξ_B respectively from the CFHT Legacy Servey data.

Shear Correlation Functions $\xi_{E,B}$

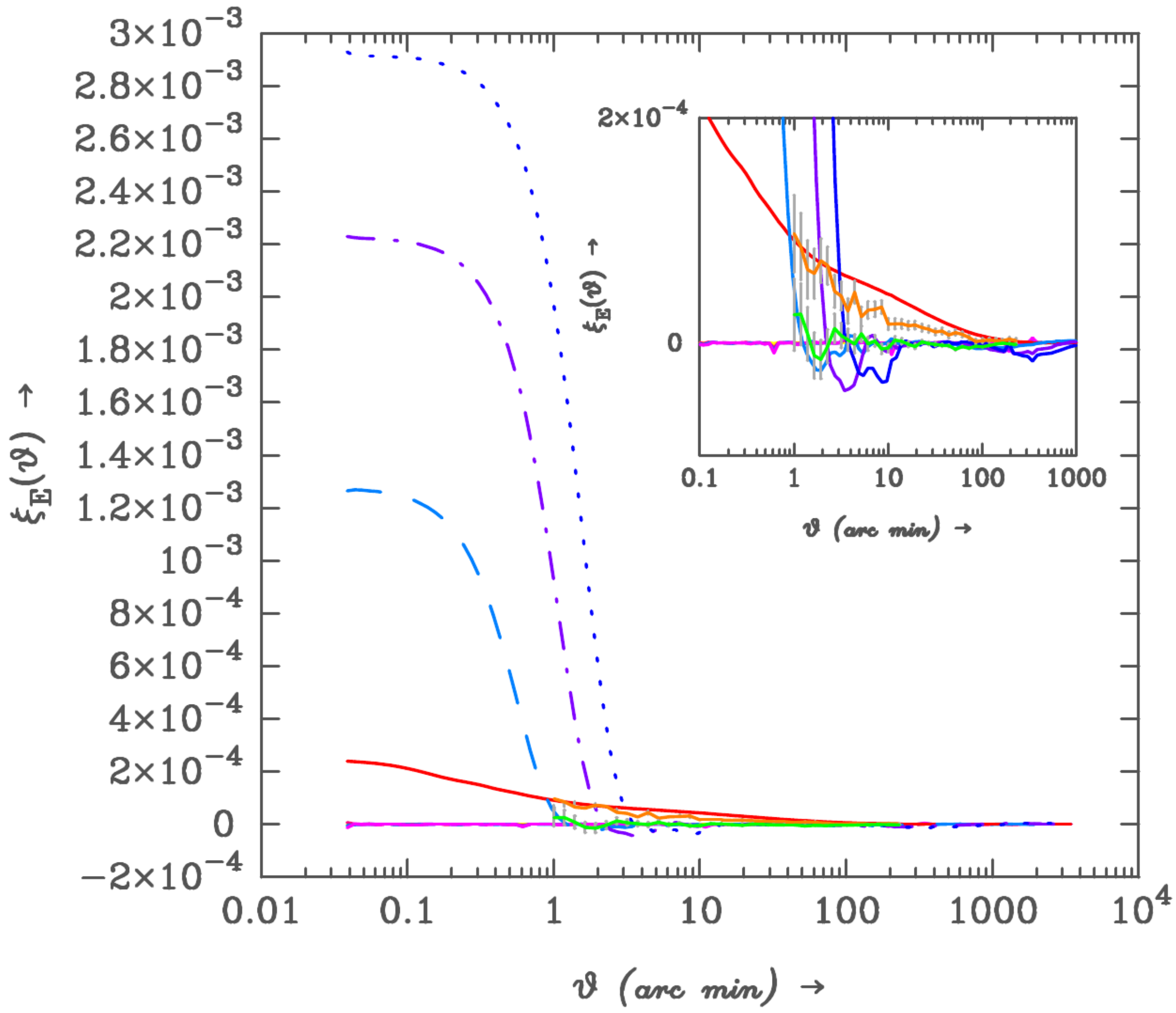

Constraints On PMF From Cosmic Shear Analysis

χ^2 Analysis

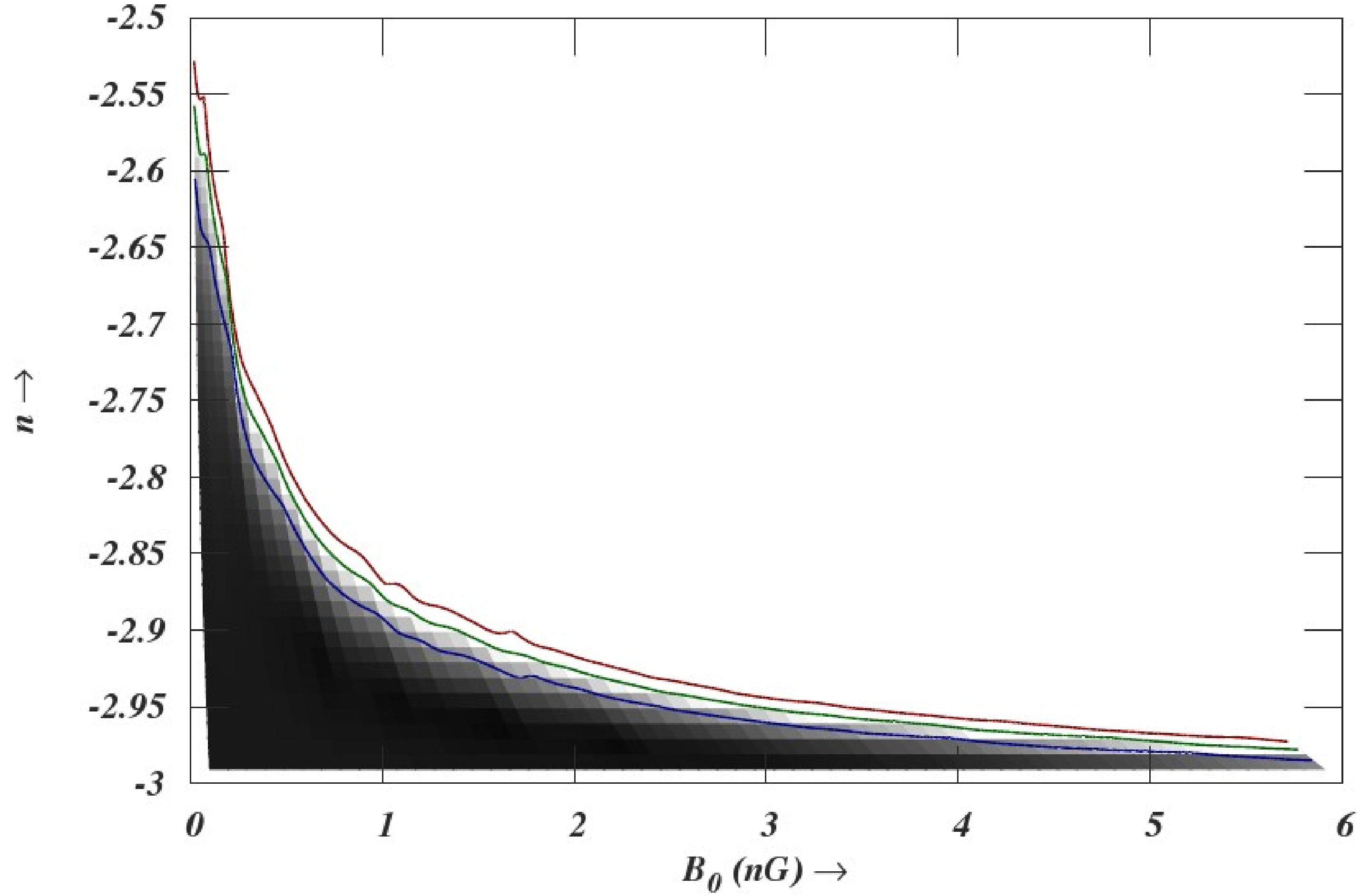

χ2 analysis : fitting of $((\xi_E)_B + (\xi_E)_{\Lambda CDM})$ against the CFHTLS data (L. Fu etal.) Contours in this figure are at 1σ, 3σ & 5σ values. Best fit values of B_0 and n are 1.5 nG and -2.96 respectively.

Constraints On PMF From Cosmic Shear Analysis

Results & Conclusions

- *Perturbations caused by large scale primordial magnetic fields at the time of last scattering, can have an appreciable effects on the matter power spectrum at small scales.*

- *We predict almost an order of magnitude stronger correlation in weak lensing signals at small angular scales (< 1 arc minute).*

- *For spectral indices $n > -2.95$ we get stronger constraints on the upper limit of primordial magnetic field strength B_0 .*

- *Future projects like SNAP are expected to have enough sensitivity to probe weak lensing signals at smaller scales (< 1 arc minute), and thus can provide us a better probe of the primodial magnetic fields.*

Probing Primordial Magnetic Fields by Studying the distribution of Mass In The Universe

4

(Constraints On Primordial Magnetic Fields Coming From The Analysis Of Lyα Observables)

Kanhaiya Lal Pandey, Shiv K Sethi

Constraints On PMF From Lyα Observables

What are Ly-α Clouds ??

- **Physical Size**: $R \approx 100h^{-1}\,\mathrm{kpc}$
- **Density**: $n_{\rm H} \approx 2.5 \times 10^{-5}\,\mathrm{cm}^{-3}$ ($N_{\rm HI} = 1 \times 10^{14}\,\mathrm{cm}^{-2}$; $\delta \approx 1$)
- **Neutral Fraction**: $n_{\rm HI}/n_{\rm HII} \approx 1.2 \times 10^{-5}$
- **Mass density**: $\Omega_{{\rm Ly}\alpha} \approx 0.015h^{-1}$
- **Temperature**: $T \gtrsim 13\,500\,\mathrm{K}$ ($b > 15\ \mathrm{km\ s^{-1}}$)
- **Metallicity**: $Z \approx 0.003 - 0.001\,Z_\odot$

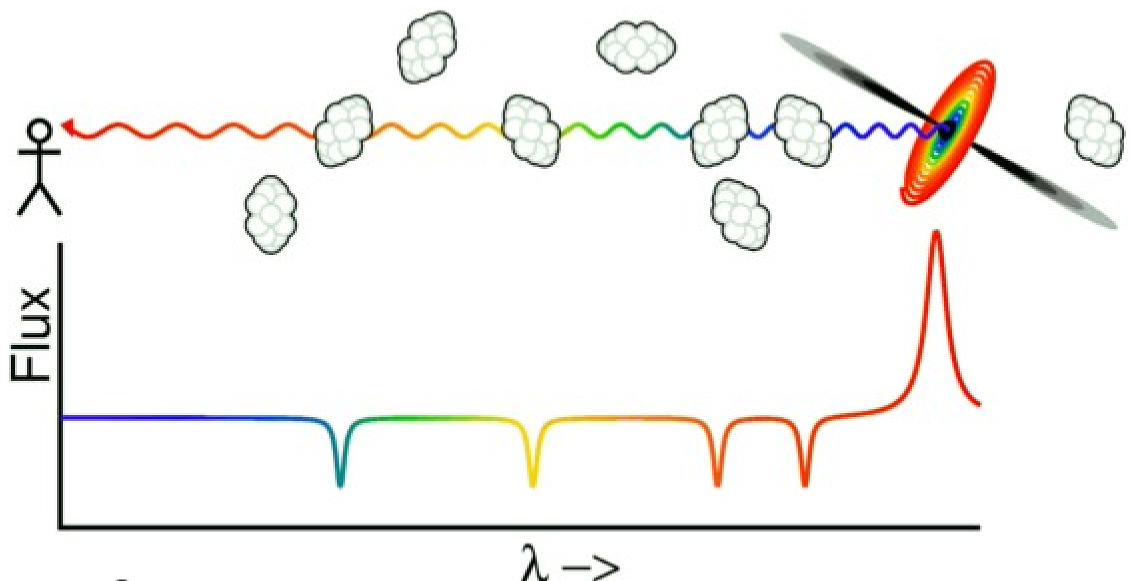

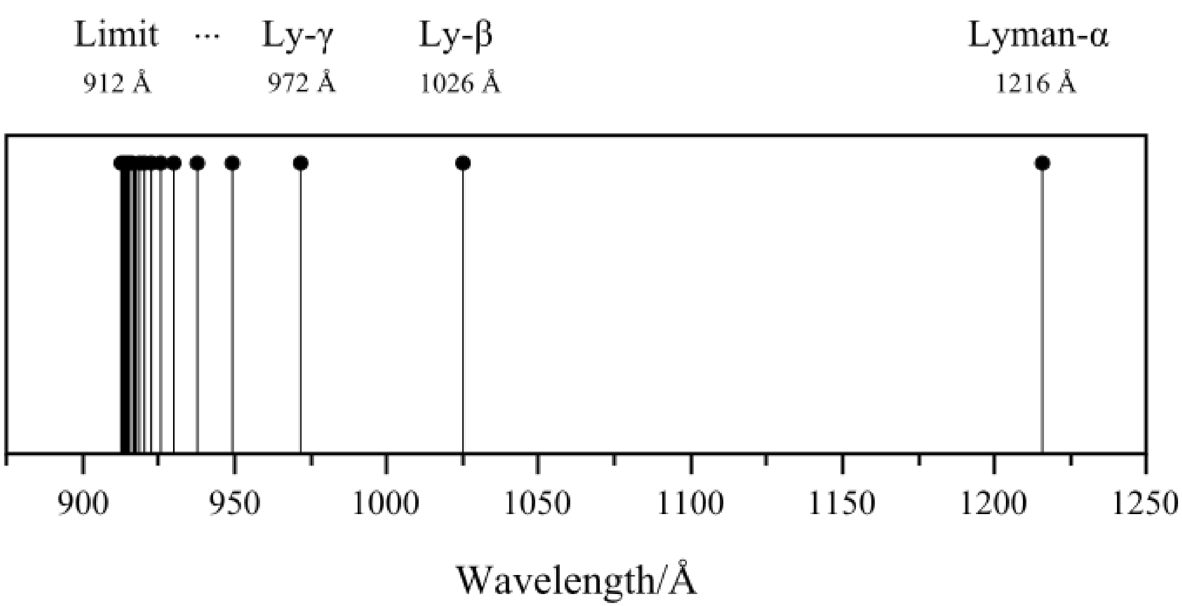

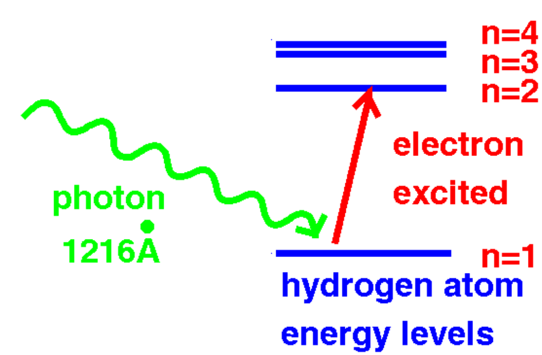

Constraints On PMF From Lyα Observables

What are Ly-α Clouds ??

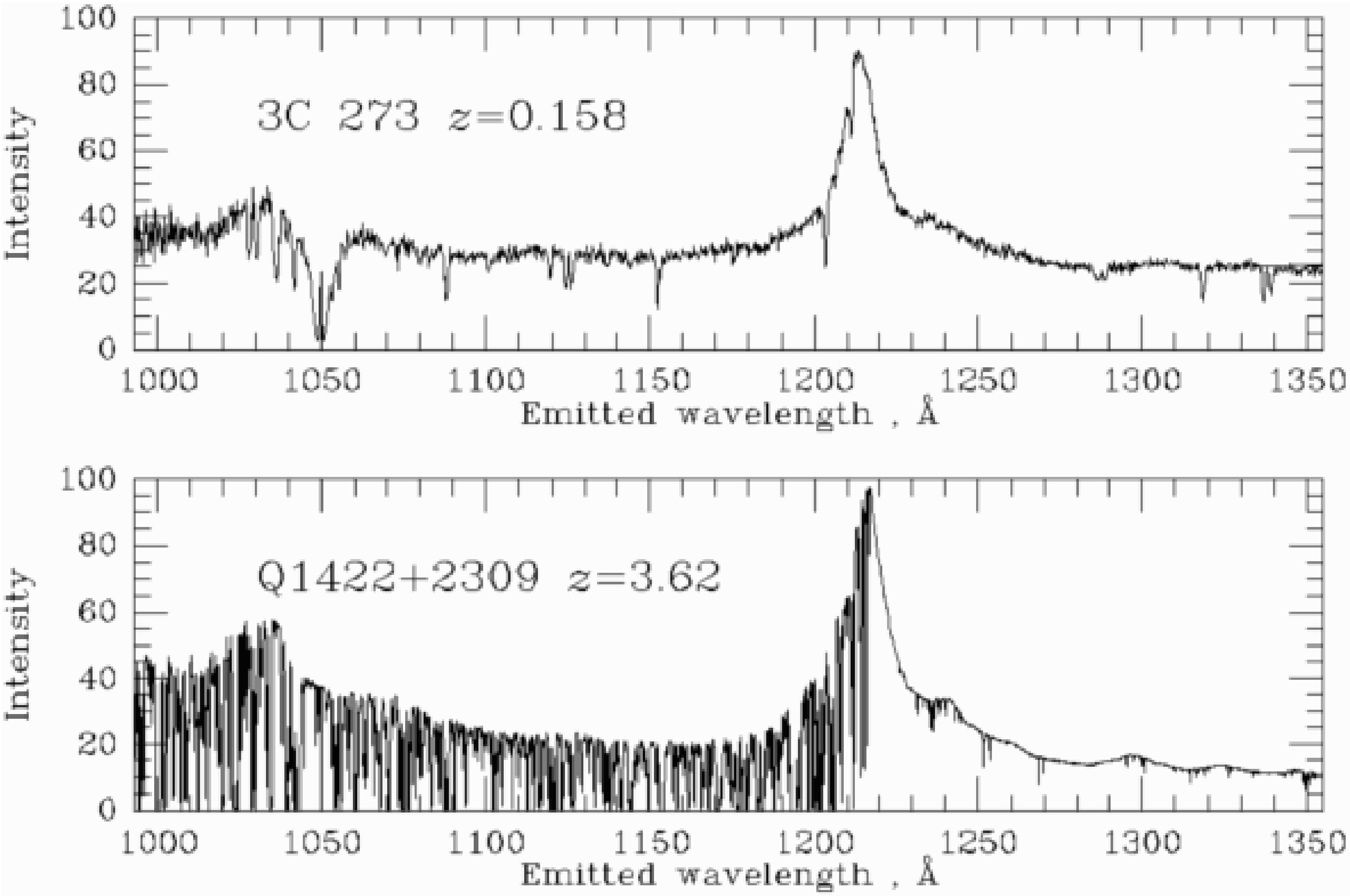

Constraints On PMF From Lyα Observables

What are Ly-α Clouds ??

Uses:

1. Matter Distribution

by studying the Lyman alpha forest we can learn about the density fluctuations in the Universe on the smallest observable scales.

2. Reionization Studies

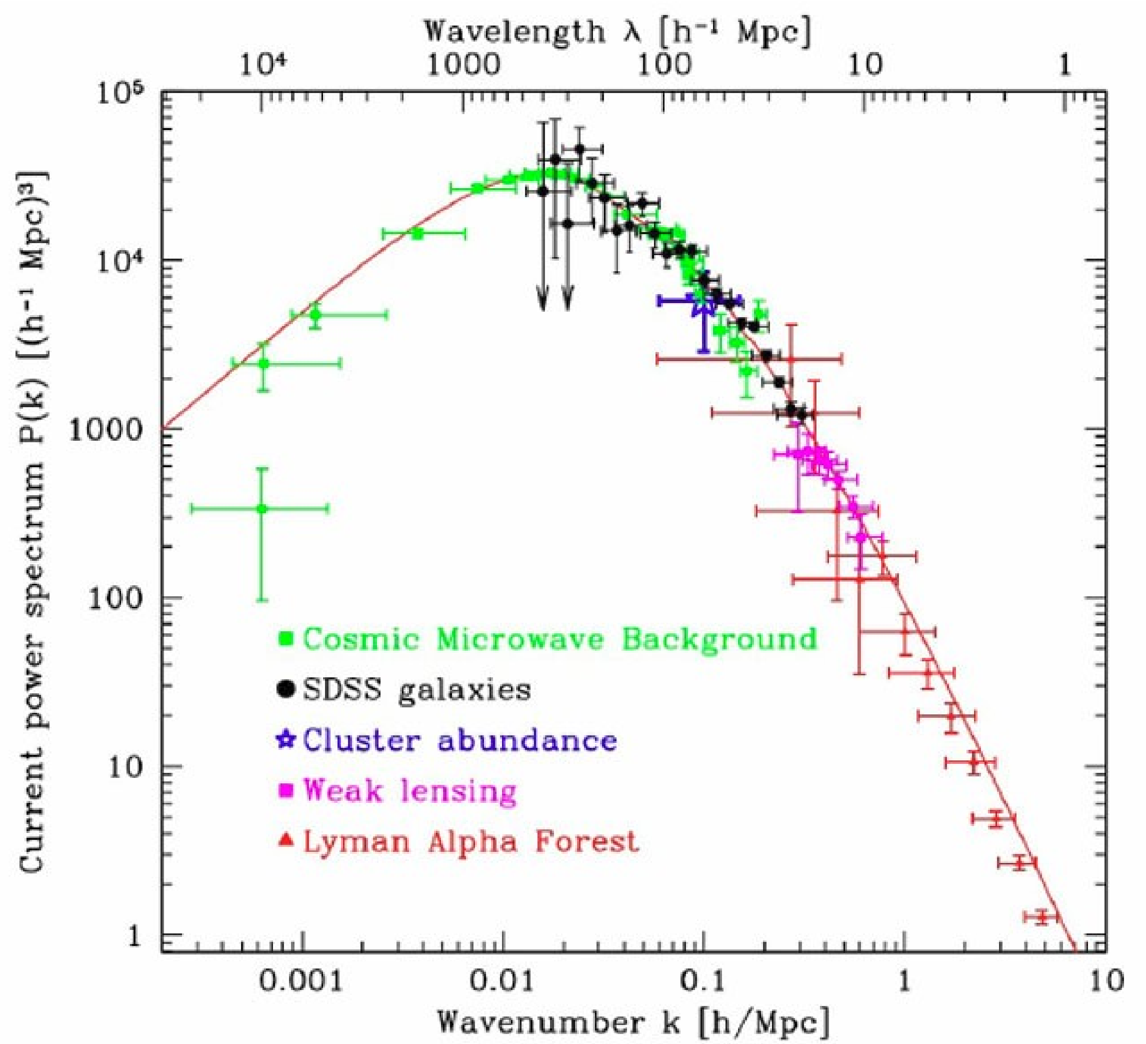

Constraints On PMF From Lyα Observables

matter distribution & primordial magnetic fields:

Primordial magnetic fields can have appreciable effects on matter distribution on the scales which are probed by Ly-Alpha clouds

- Ly-Alpha clouds can be a probe to primordial magnetic fields

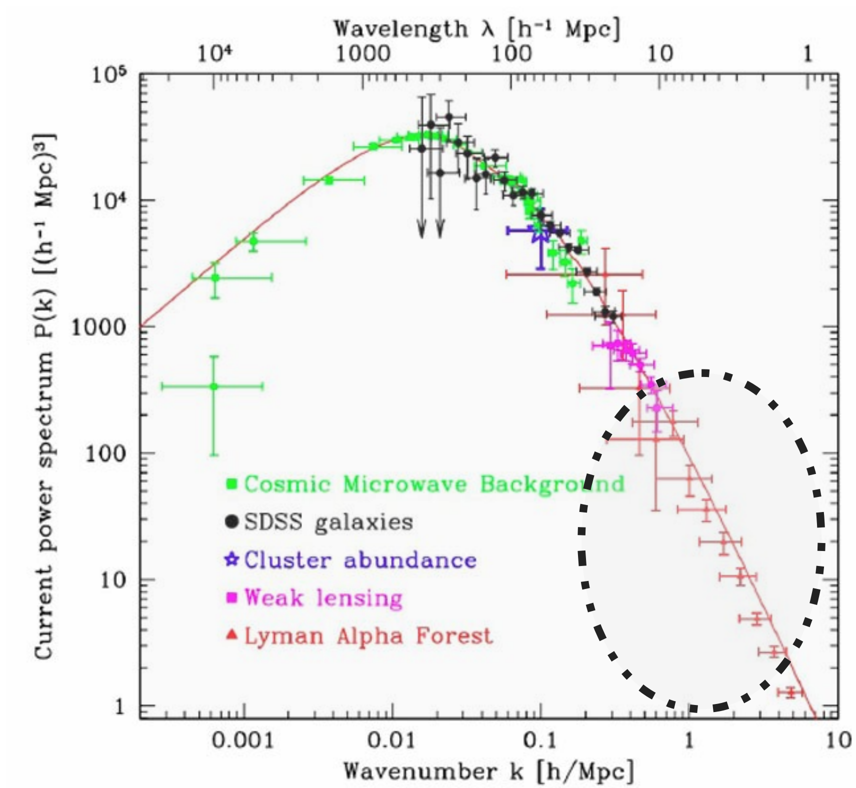

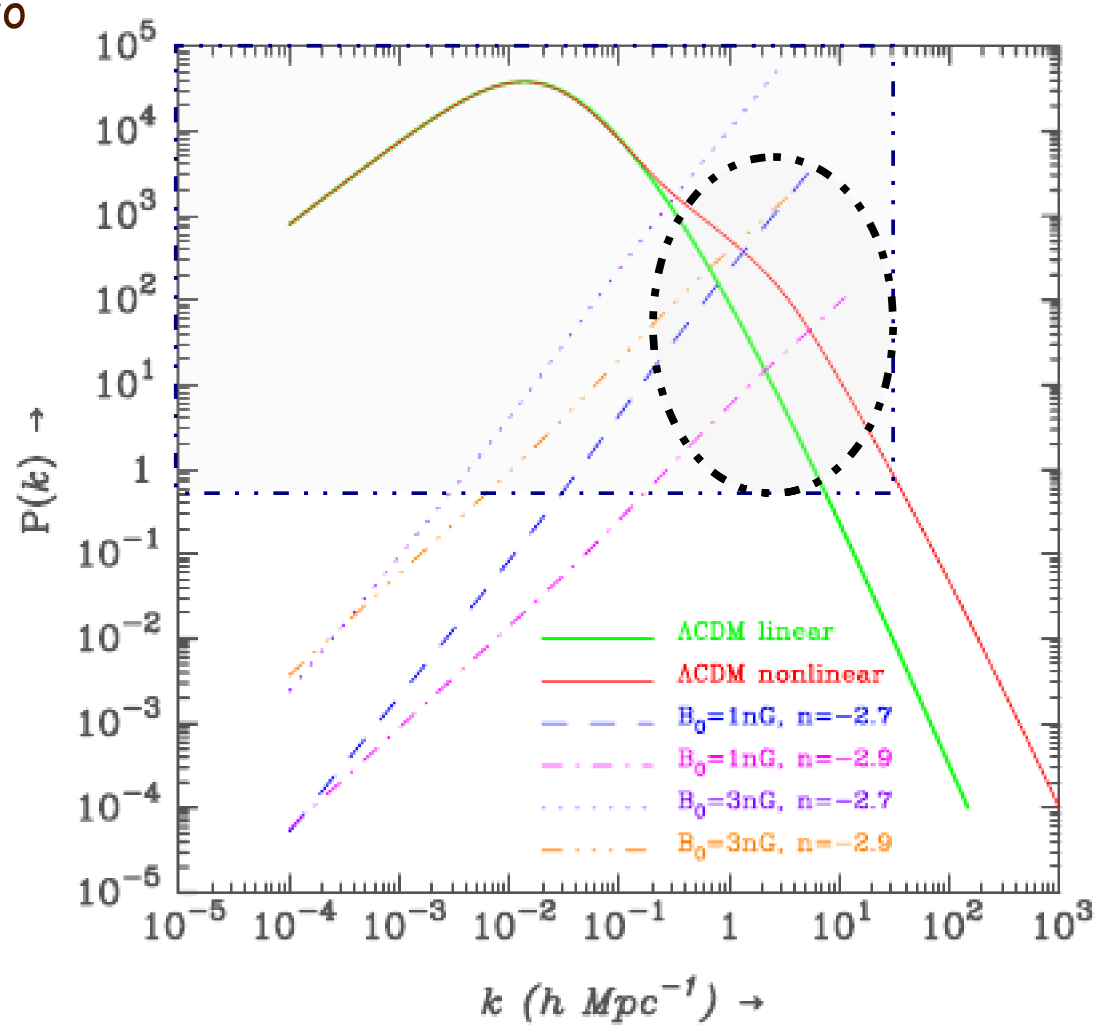

Constraints On PMF From Lyα Observables

Ly-α Clouds → Matter Power Spectrum

Ly-Alpha Forest Spectra

↓

Transmitted flux [$F = \exp(-\tau)$]

↓

Opacity $\tau \propto (\rho_b^{1D})^{\beta}$

↓

$\rho_b^{1D} \longrightarrow \rho_b^{3D}$

↓

$P(k)$

arbitrary normalization

normalize by matching independent observations

Croft etal. 1999

Constraints On PMF From Lyα Observables

Our Plan

3d Matter Power Spectrum (infl + pmf)

↓

simulate Ly-Alpha Clouds

↓

calculate opacity of Ly-Alpha clouds (τ, τ_{eff})

↓

compare with the observations → bounds on pmf

Constraints On PMF From Lyα Observables

Matter Power Spectrum → Ly-α Clouds

1: 3d-PS → 1d-PS

3d Baryonic Matter Power Spectrum (infl / pmf)

3d Matter Power Spectrum (infl / pmf)

$$P_B^{(3)}(k,\, z) = \frac{P_{\rm DM}^{(3)}(k,\, z)}{[1 + x_b^2(z) k^2]^2}$$

(thermal / magnetic) Jenas Scale

$$P_B^{(1)}(k,\, z) = \frac{1}{2\pi} \int_{|k|}^{\infty} dk' k' P_B^{(3)}(k',\, z)$$

$$P_v^{(1)}(k,\, z) = \dot{a}^2(z) k^2 \frac{1}{2\pi} \int_{|k|}^{\infty} \frac{dk'}{k'^3} P_B^{(3)}(k',\, z)$$

$$P_{Bv}^{(1)}(k,\, z) = i\dot{a}(z) k \frac{1}{2\pi} \int_{|k|}^{\infty} \frac{dk'}{k'} P_B^{(3)}(k',\, z)$$

Constraints On PMF From Lyα Observables

Matter Power Spectrum → Ly-α Clouds

2 : 1d-PS → LOS density & velocity fluctuation field

The density (δ_b (k, z)) and velocity (v (k , z)) fields in one dimension are two correlated Gaussian random fields (the correlation is given by the density–velocity power spectrum P_{bv});

we use the inverse Gram–Schmidt procedure to simulate them

$$(P^{1D}_{bb},\ P^{1D}_{bv},\ P^{1D}_{vv})$$

↓

$$\delta_b^{1D}(k,z)\ \&\ \delta_v^{1D}(k,z)$$

↓

$$\delta_b^{1D}(x,z)\ \&\ \delta_v^{1D}(x,z)$$

Constraints On PMF From Lyα Observables

Matter Power Spectrum → Ly-α Clouds

3 : Calculating LOS log-normal density field

to take into account the effect non-linear evolution of density field

density & velocity fields

↓

log-normal density fields

↓

Ly-Alpha Clouds

$\delta_B^{1D}(infl) + \delta_B^{1D}(pmf)$

$$n_B(x, z) = A e^{\delta_B(x, z)}$$

$$A = \frac{n_0(z)}{\langle e^{\delta_B(x, z)} \rangle}$$

Bi & Davidson, 1995

Constraints On PMF From Lyα Observables

Calculation of Ly-α Opacity (τ) -

The number density of neutral hydrogen, n_{HI}, can be computed by solving ionization equilibrium equation,

$$\alpha(T)n_p n_e = \Gamma_{ci}(T)n_e n_{\mathrm{H\,I}} + J n_{\mathrm{H\,I}}$$

Baryonic density field
(n_b)
↓
Neutral hydrogengen density
Fields (n_{HI})

$$n_{\mathrm{H\,I}}(x, z) = \frac{\alpha[T(x, z)]n_B(x, z)}{\alpha[T(x, z)] + \Gamma_{ci}[T(x, z)] + J(z)/[\mu_e n_B(x, z)]}$$

$$T(x, z) = T_0(z)\left[\frac{n_B(x, z)}{n_0(z)}\right]^{\gamma - 1}$$

$T_0(z)$ ⇒ temperature of the IGM at the mean density ; $4000 < T_0 < 15{,}000$ K

γ ⇒ polytropic index for the IGM ; $1.3 < \gamma < 1.6$

α(T), Γci (T), and J (z) are the recombination rate, collisional ionization rate, and photoionization rates in the IGM.

Constraints On PMF From Lyα Observables

Calculation of Ly-α Opacity (τ) -

$$\tau(\nu) = \int n_{\mathrm{H\,I}}(t)\sigma_a\left(\frac{\nu}{a}\right)dt$$

ν is the observed frequency, which is related to redshift z by $z \equiv (\nu_a / \nu) - 1$, and ν_a is the Lyα frequency at rest. The absorption cross section σ_a is given by

$$\sigma_a = \frac{I_a}{b\sqrt{\pi}} V\left(\alpha, \frac{\nu - \nu_a}{b\nu_a} + \frac{v}{b}\right)$$

where parameter $b = (2kT / m_p)^{1/2}$ is the velocity dispersion and v(x) is the peculiar velocity field, $\alpha \equiv 2\pi e^2 \nu_a / 3m_e c^3 b = 4.8548 \times 10^{-8} / b$, $I_\alpha = 4.45 \times 10^{-18}$ cm^{-2}, and V(α,..) is the Voigt function.

Constraints On PMF From Lyα Observables

Calculation of Ly-α Opacity (τ) -

The combination of the above mentioned effects yields (Croft et al. 1998)

$$\tau \propto \rho_b^2 T^{-0.7} = A(\rho_b/\bar{\rho}_b)^{\beta},$$

$\beta = 2 - 0.7(\gamma - 1)$

$$A = 0.946\left(\frac{1+z}{4}\right)^6\left(\frac{\Omega_b h^2}{0.0125}\right)^2\left(\frac{T_0}{10^4\ \mathrm{K}}\right)^{-0.7} \times \left(\frac{\Gamma}{10^{-12}\ \mathrm{s}^{-1}}\right)^{-1}\left[\frac{H(z)}{100\ \mathrm{km\ s^{-1}\ Mpc^{-1}}}\right]^{-1}$$

But τ is not an observable quantity what we observe is τ_{eff} :

$$\tau_{\mathrm{eff}}(z) = -\log\left[\langle \exp(-\tau) \rangle\right]$$

Constraints On PMF From Lyα Observables

Findings -

redshift evolution of <τ> (uncorrelated case)

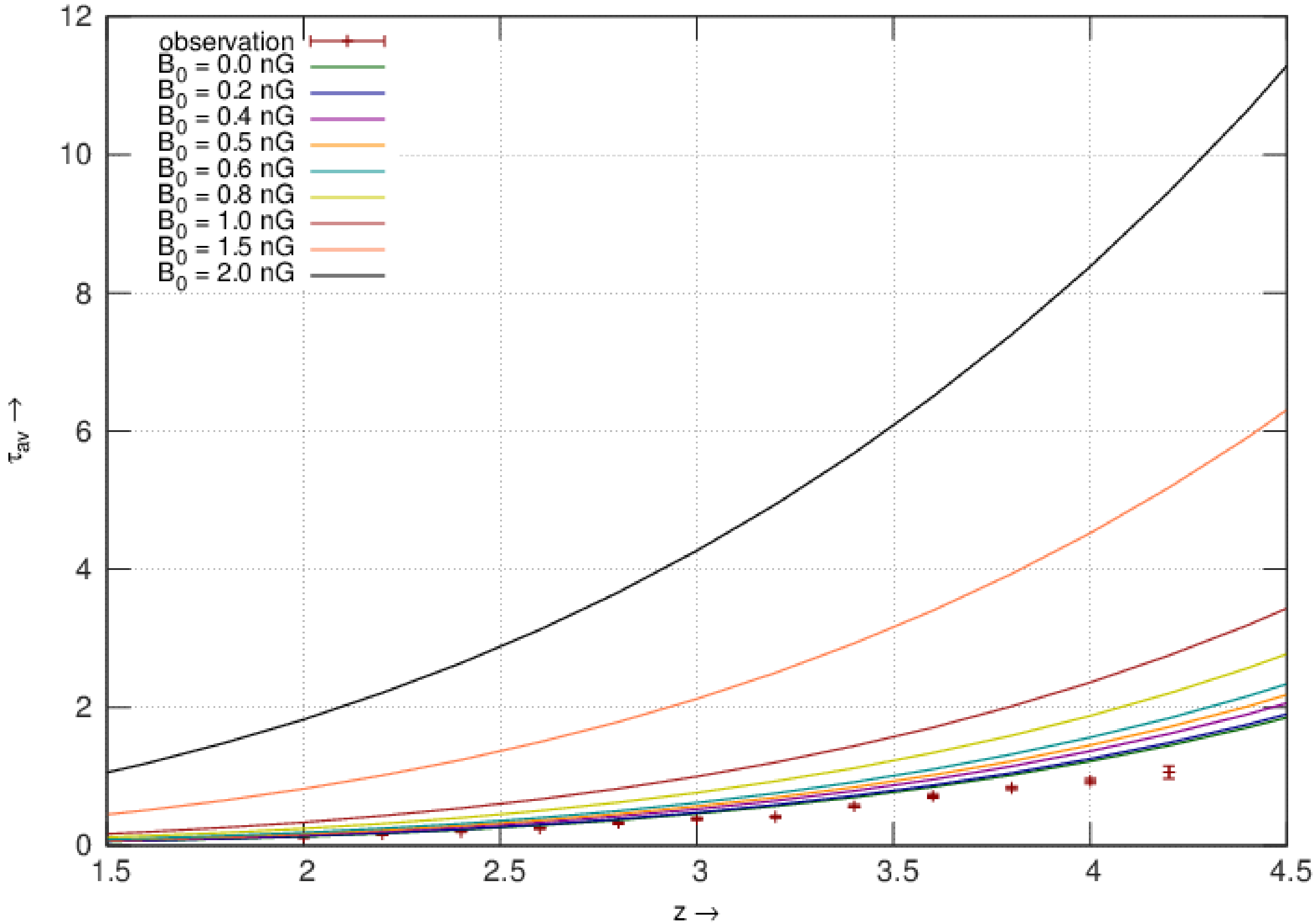

Constraints On PMF From Lyα Observables

Findings -

redshift evolution of <τ> (correlated case)

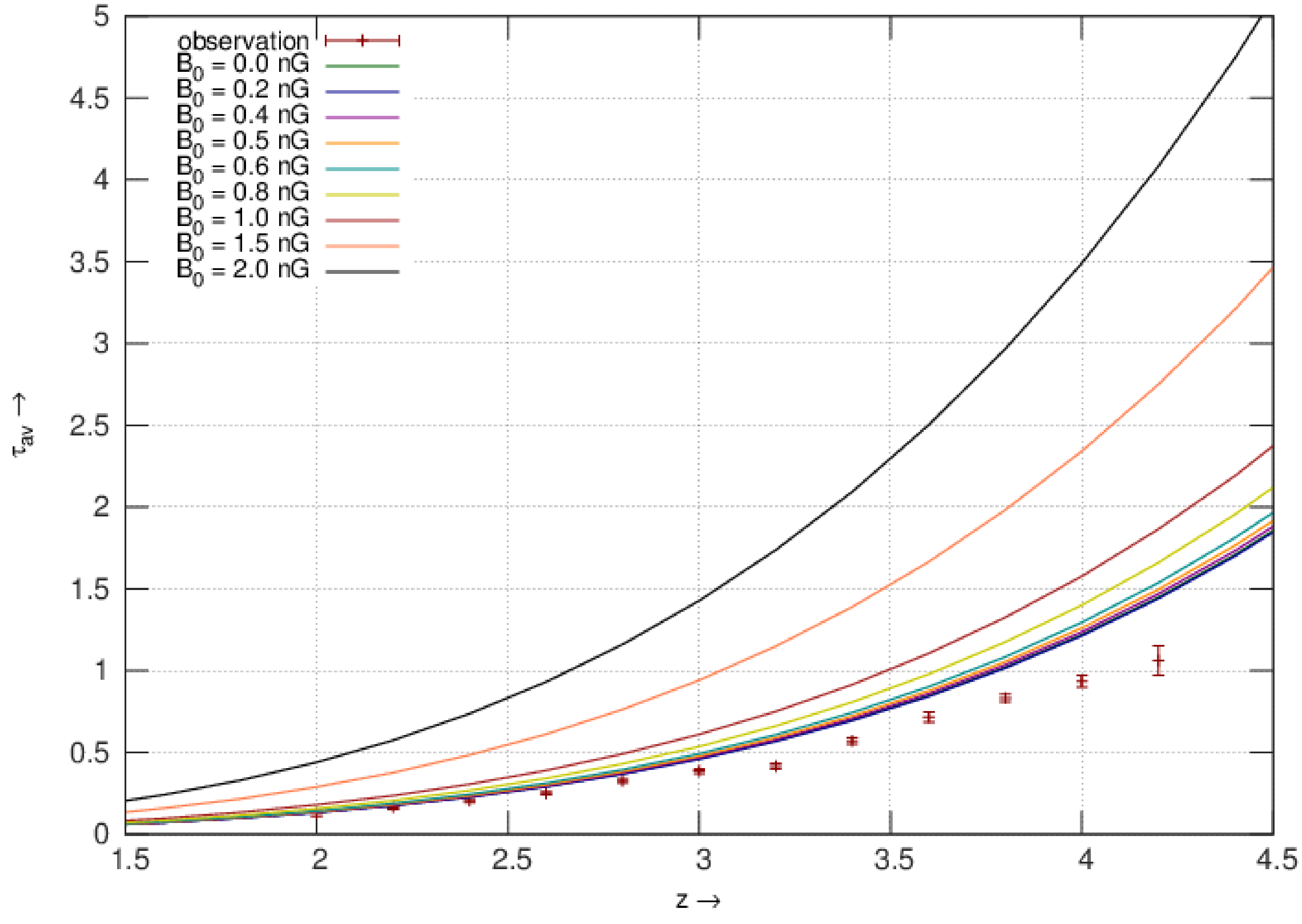

Constraints On PMF From Lyα Observables

Findings -

redshift evolution of τ_{eff} (uncorrelated case)

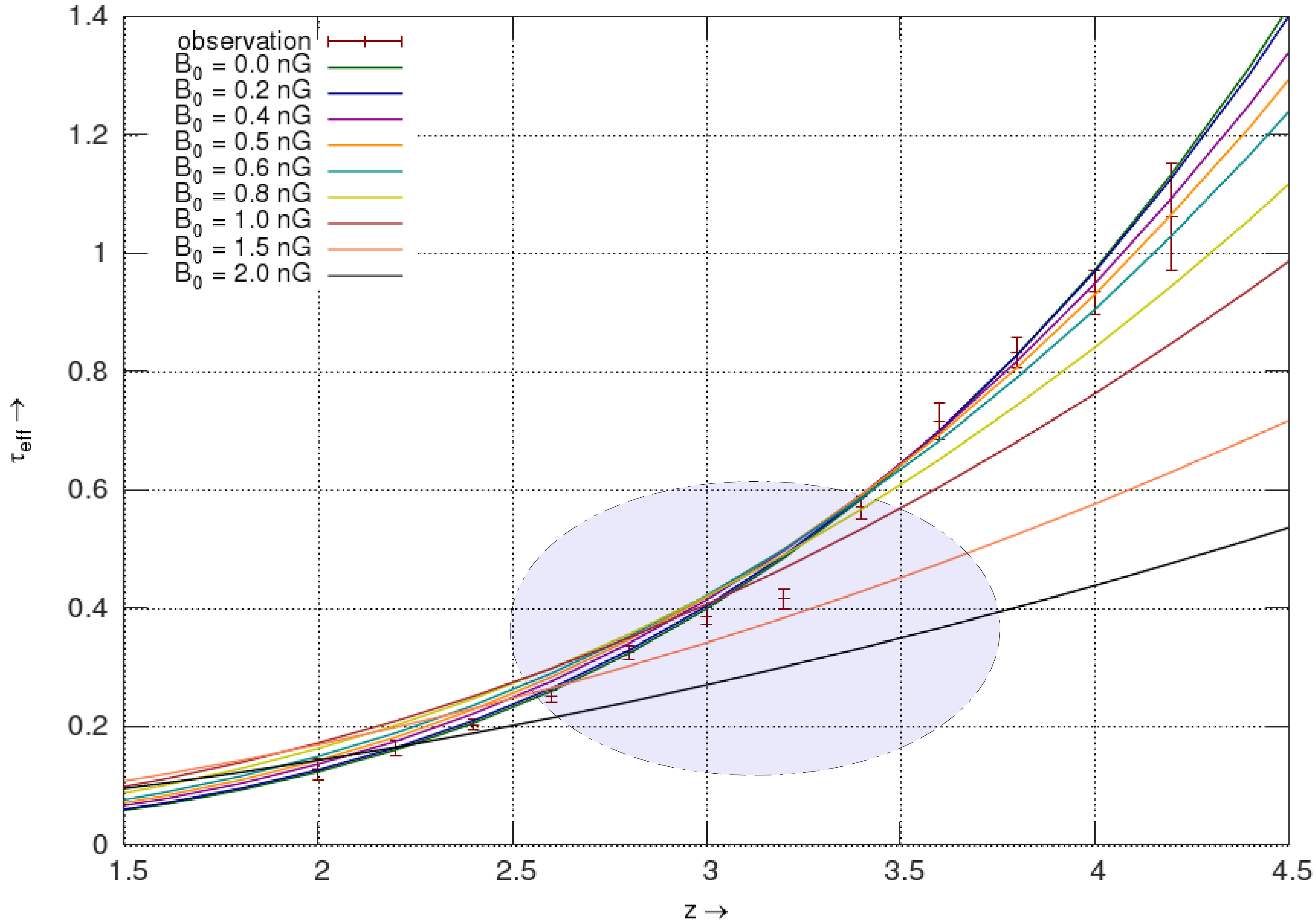

Constraints On PMF From Lyα Observables

Findings -

redshift evolution of τ_{eff} (correlated case)

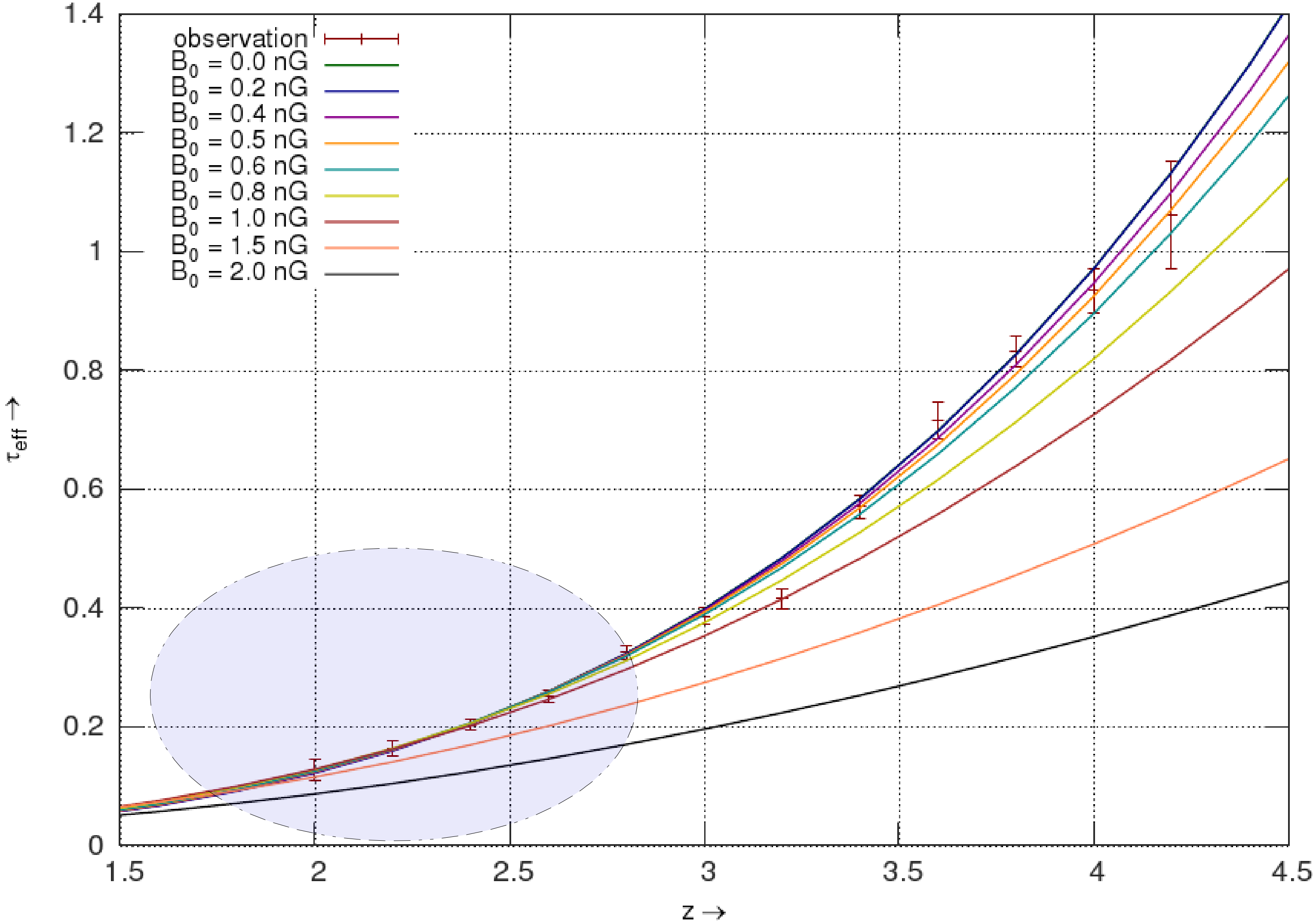

Constraints On PMF From Lyα Observables

Findings **-**

χ^2 test 1, 3 & 5 σ contours

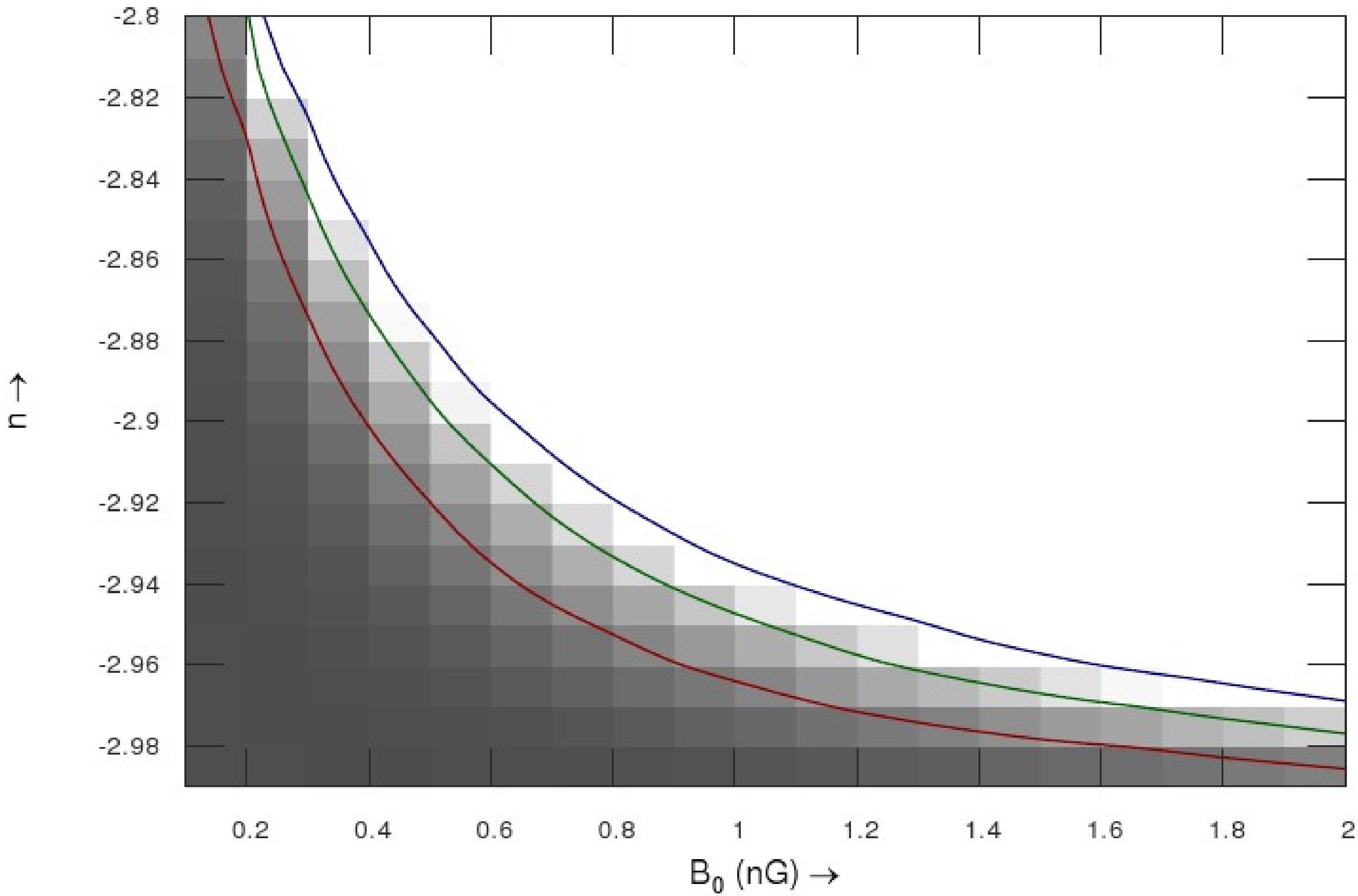

Constraints On PMF From Lyα Observables

Findings -

χ^2 analysis 1, 3 & 5 σ contours

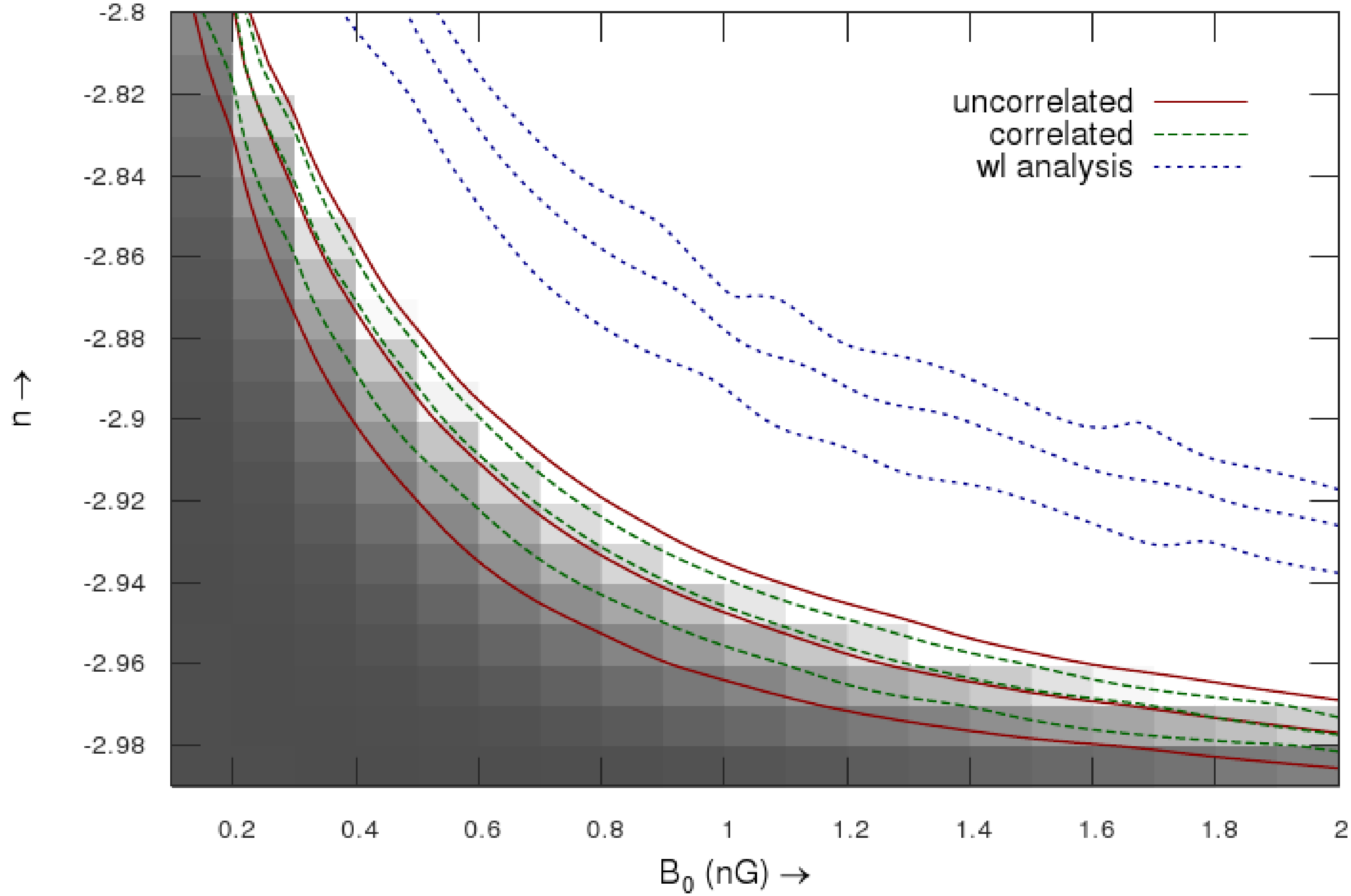

Constraints On PMF From Lyα Observables

Results & Conclusions

- *In this work we have simulated one dimensional distribution of Lyα absorbers along the line of sight and calculated effective Lyα opacity as function of redshift.*

- *We have calculated bounds on primordial magnetic field, which turned out to be even stronger than our previous estimates ($B0 \sim 0.2 - 0.3$ nG for $nB = -2.8$ with the confidence level of 5σ) and are the best known bounds on primordial magnetic fields till date.*

- *In this analysis we have considered two cases, one when the magnetic field induced perturbations are uncorrelated with inflationary perturbations, and the other is when they are correlated, though the final results (bounds on B0) are not very different for both the cases.*

An Overview

~

(Main Results)

This Thesis : An Overview

Main Results (1 – 2)

- *Dissipation of sufficiently strong magnetic fields (> 3.5 nG) via ambipolar diffusion or decaying turbulence can lead to heating of the collapsing gas and can compansate for the H_2 cooling. In this scenario one can have sufficently massive seed black holes by the redshift z ~ 20–25, which can grow to SMBHs of masses around $10^9 M_\odot$ by the time of redshift z ~ 6.*

- *By the redshift z ~ 10 (reionization) number of magnetic field ($B_0 \sim 1$ nG) induced halo collapse are much more than the same for pure ΛCDM model.*

An Overview

Main Results (3 – 4)

- *From our weaklensing shear analysis we get strong (for nearly scale invariant model, n_B = -2.9 B_0 ~ 1.5 nG, @ 5 σ CL) bounds on primordial magnetic fields. These bounds are stronger than the bounds calculated using other CMB analysis.*

- *We get the strongest known bound on primordial magnetic fields from our Lyα analysis. (n_B = -2.9, B_0 ~ 0.6 nG, @ 5 σ CL)*

Thanks . .

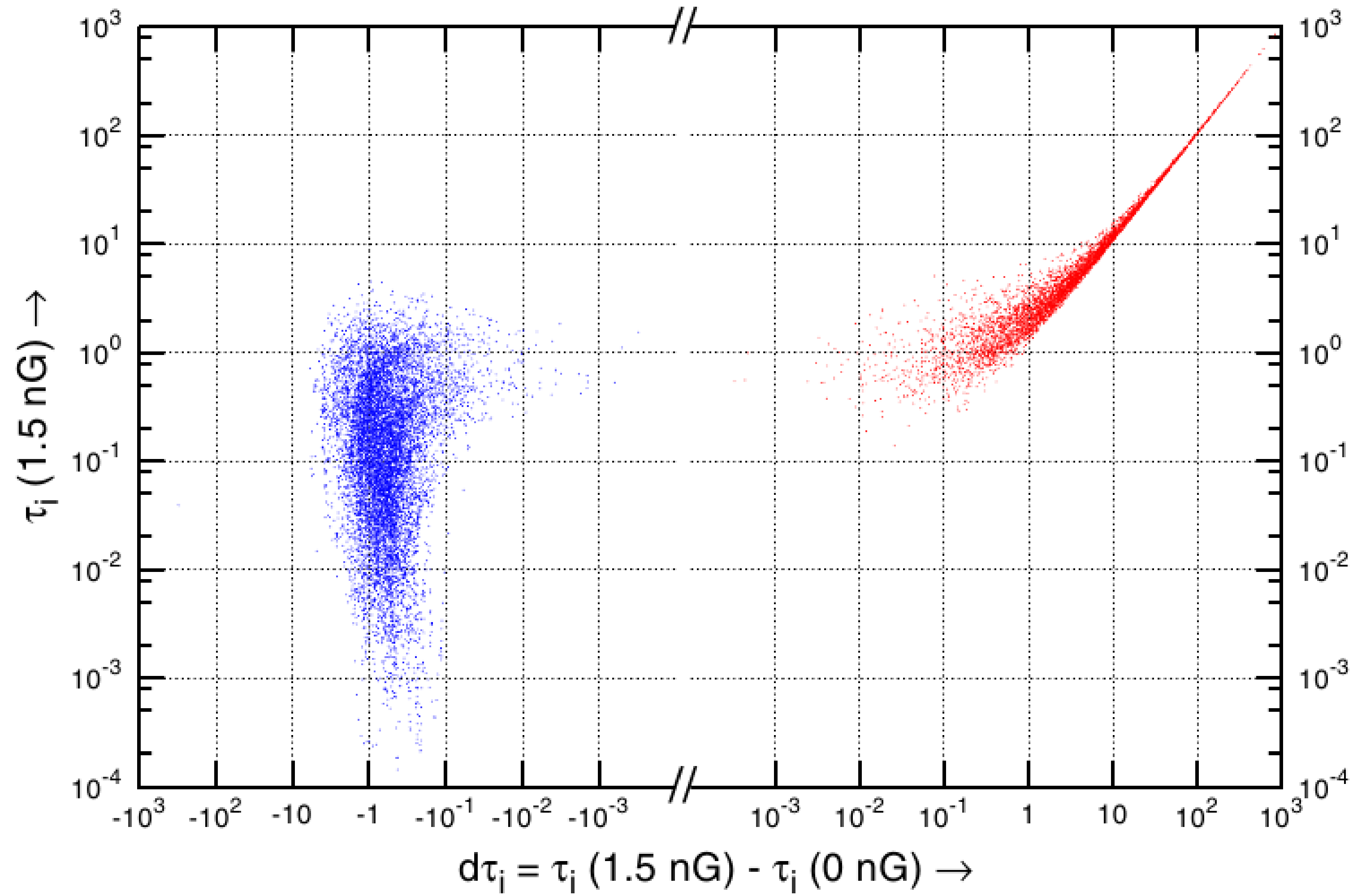

Figure 4. Distribution of $\tau_i(1.5\,\mathrm{nG})$ vs. $d\tau_i(= \tau_i(1.5\,\mathrm{nG}) - \tau_i(0\,\mathrm{nG}))$ at redshift $z = 4$.
(A color version of this figure is available in the online journal.)